I&EC research
Industrial & Engineering Chemistry Research

pubs.acs.org/IECR
Article

Optimizing Emissions Reduction in Ammonia–Ethylene Chemical Clusters: Synergistic Integration of Electrification, Carbon Capture, and Hydrogen

Published as part of Industrial & Engineering Chemistry Research special issue "Marco Mazzotti Festschrift".

Julia L. Tiggeloven, André P. C. Faaij, Gert Jan Kramer, and Matteo Gazzani*

Cite This: *Ind. Eng. Chem. Res.* 2025, 64, 4479–4497

Read Online

ACCESS | Metrics & More | Article Recommendations | Supporting Information

ABSTRACT: The transition of the chemical industry to net-zero CO_2 emissions presents several significant challenges, due to the presence of carbon as material feedstock, the capital-intensive nature of plants, the interdependence of multiple processes within industrial clusters, and the availability of low-carbon electricity, hydrogen, and CO_2 transport and storage. To obtain an effective plan for reducing emissions, a comprehensive modeling approach that accounts for the dynamics of clusters and their interactions with the broader energy system is needed. In light of the aforementioned considerations, the present study develops and applies a mixed-integer linear programming (MILP) model with a one-year hourly resolution to optimize technology selection and operation in two existing ammonia-ethylene clusters. The findings show that significant emission reduction is possible with close-to-market technologies that bridge electrification, green hydrogen, and carbon capture and storage, yet reaching zero emission is not possible. Moreover, the optimal CO_2 reduction strategies are highly cluster-specific and contingent upon the availability of a critical infrastructure. For instance, emissions can increase by up to 118% in the absence of a CO_2 transport and storage infrastructure, because separated CO_2 from reformer syngas cannot be stored or further utilized. While process integration can improve cost-effective CO_2 mitigation, reducing costs by 9−%11% and emissions by 29%−54%, it also limits operational flexibility. The developed framework offers a valuable tool for identifying cluster designs and robust CO_2 emission reduction strategies.

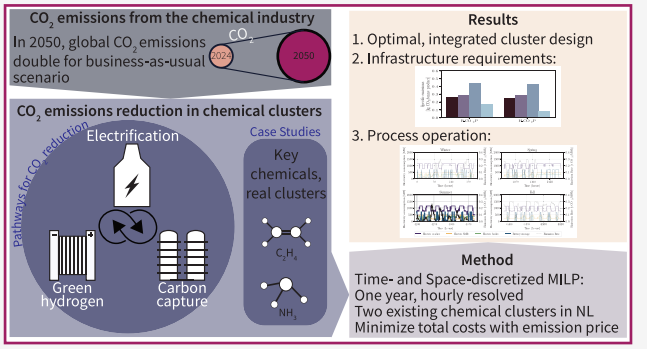

INTRODUCTION

In *Moby Dick*, a novel by Herman Melville, Captain Ahab relentlessly hunts a gigantic white whale. His quest is more than just a physical challenge: it symbolizes a deeper struggle, an exploration of the human's capacity to confront and sometimes be consumed by radical challenges. Few would disagree with saying that the chemical industry is confronted with a radical, existential crisis when trying to achieve net-zero CO_2 emissions. Achieving zero scope one, two, and three CO_2 emissions by 2050 requires a coordinated realization of multiple transformations, above all (i) using renewable electricity to run as many processes as possible (i.e., pursue electrification), and (ii) switching from fossil-based feedstocks to CO_2-neutral hydrogen and carbon.[1] When adding that the transformation needs to happen in a world-competing market and that it will require enormous flows of fresh capital, it becomes evident that the chemical industry is likely the most challenging sector to become CO_2-neutral. At the same time, few would disagree with saying that the chemical industry—maybe inspired by Captain Ahab—should tackle the net-zero challenge like an existential crisis, and less like a run to be the last fossil fuel user. The chemical industry transition must be successful to avoid all other industrial sectors from failing the target.

When looking at global CO_2 emissions, the chemical industry accounts for 5.6 Gt, or ∼10%.[2] Notably, the production of ammonia and high-value chemicals like ethylene, propylene, benzene, toluene, and mixed xylenes represents over 70% of the emissions from the chemical industry.[3] These key chemicals are typically produced in large integrated chemical clusters, which are designed to optimize energy and material efficiency and minimize CO_2 emissions. However, the significant interdependence within these clusters may add further resistance to the adoption of the new technologies required for substantial

Received: October 8, 2024
Revised: February 1, 2025
Accepted: February 2, 2025
Published: February 14, 2025

https://doi.org/10.1021/acs.iecr.4c03817
Ind. Eng. Chem. Res. 2025, 64, 4479−4497

emission reductions. Furthermore, while numerous opportunities exist for emission mitigation in the chemical industry,[4] they involve a significant increase in low-carbon electricity demand and require a robust CO_2 transport and storage infrastructure. Despite governmental ambitions to ensure sufficient renewable electricity generation, grid capacity, and a CO_2 transport infrastructure in the near future, these plans might be overly ambitious. Consequently, certain industrial decarbonization strategies might prove infeasible or even counterproductive, potentially leading to increased emissions. Hence, selecting the most appropriate decarbonization technologies in the chemical industry is a complex effort that requires a comprehensive modeling approach, which must include a detailed representation of the chemical cluster, its downstream processes, and the interaction with the surrounding energy and material system (e.g., cost and availability of renewable electricity and CO_2 transport and storage infrastructure, electric grid connection capacity, space available for new installations).

While substantial literature exists on modeling and optimizing industrial clusters, these studies primarily focus on enhancing synergies, renewable electricity uptake, and energy efficiency (see, e.g., the work of Hackl and Harvey[5] and Theo et al.[6]). However, deep decarbonization in the chemical industry requires more than just improved energy efficiency through process integration. Various studies have qualitatively explored the opportunities and challenges of deep "decarbonization" in chemical clusters.[7−10] The resulting key challenges include (1) addressing technological incompatibilities among different emission reduction pathways, (2) maintaining optimized integrated systems during the replacement of existing installations, and (3) managing the complexities of multiple decision-makers without a unified long-term vision. These challenges, rooted in uncertainties and unknowns, highlight the need for quantitative assessments to provide deeper insights into optimal strategies for achieving a deep CO_2 reduction in chemical clusters.

Most quantitative studies on the optimal selection of CO_2 reduction technologies in industrial clusters focus on a single decarbonization route. For example, Gunawan et al.[11] developed a generalized expression for carbon capture (CC) and storage costs, optimizing a shared CO_2 infrastructure for a 22-facility cluster. Küng et al.[12] are developing an open-source toolkit to identify net-zero pathways in industrial clusters, primarily focusing on CC. Namazifard et al.[13] are using a MILP model to design a minimum-cost hydrogen infrastructure for industrial decarbonization at a detailed spatiotemporal resolution. Ibrahim and Al-Mohannadi[14] have designed an optimal hydrogen supply chain considering CC for a new hydrogen production cluster (rather than for an existing chemical cluster). Research on electrifying the chemical industry focuses on integrating processes with variable renewable electricity and the resulting dynamic operation. For example, Giannikopoulos et al.[15] explore combining a wind farm and battery system for thermal electrification of a chemical process network using multi-objective MILP optimization. Wajeh et al.[16] optimized the design and flexible operation of an electrified biodiesel production process through nonlinear optimization.

While these models offer detailed technotemporal and spatial resolutions, they do not explore the potential of combining different decarbonization routes and different clusters, which is crucial for deep emission reduction. Additionally, they do not include downstream processes in their analyses. Conversely, Samadi et al.,[17] Fleiter et al.,[18] Berghout et al.,[19] and Yáñez et al.[20] incorporated multiple decarbonization routes, with Samadi et al.,[17] Berghout et al.,[19] and Yáñez et al.[20] also considering downstream processes. However, these studies build upon (time-independent) simulations rather than optimization, thus limiting the capacity to identify synergies between different industry types and their operation.

In summary, there is a lack of studies that use time- and space-resolved mathematical optimization to integrate multiple decarbonization technologies in chemical clusters while accounting for the variability in resource availability such as fluctuating electricity prices, grid capacity limits, CO_2 transport and storage costs, and downstream energy and material demand. This study addresses the gap using an MILP model to optimize technology selection and (flexible) operation to reduce emissions in real ammonia−ethylene chemical clusters under fluctuating boundary conditions. By simultaneously considering two key chemical industry types and their multiple alternative processes—electrification, carbon capture, and green hydrogen—this study quantifies the challenges and benefits of integrated industrial clusters in reducing emissions. We do this by employing a one-year hourly resolution for two existing Dutch chemical clusters.

This study addresses the existing knowledge gap by providing novel methodological and application contributions. From a methodological point of view, we analyze the transition of ammonia−ethylene clusters, including their process interconnections and connection to the national infrastructures, using time- and space-discretized mixed integer linear programming; moreover, we develop constraints to simulate ramp-up/down and transient operation of chemical processes with design days. From an application perspective:

(i) We optimize cost-optimal emission abatement strategies for ammonia−ethylene chemical clusters at two locations, including electrification (e.g., electric cracking and reforming), green hydrogen, and carbon capture and storage, which allows evaluating new technologies from a system perspective (e.g., how to reuse cracker gas with electric crackers).

(ii) We assess the role of cluster integration and boundary conditions, such as fluctuating electricity prices, grid capacity limits, and the availability and costs of CO_2 transport and storage infrastructure.

(iii) We evaluate the impact of flexibility in alternative technologies with detailed linear technology performance models.

To do so in a computationally efficient manner, i.e., where problems can be resolved on regular computers with commercial solvers, we further discuss how complexity can be handled and reduced, for example, employing a combination of design days and full hourly resolution and by extending ramping constraints to the resulting time framework.

This work is organized as follows: the second section describes the research framework, the chemical clusters considered, and the technology cost and performance data. The third section explains the optimization framework, the technology constraints, and the application of time series aggregation in combination with ramping constraints. Then, the results are presented, followed by a discussion and conclusions and recommendations.

https://doi.org/10.1021/acs.iecr.4c03817
Ind. Eng. Chem. Res. 2025, 64, 4479−4497

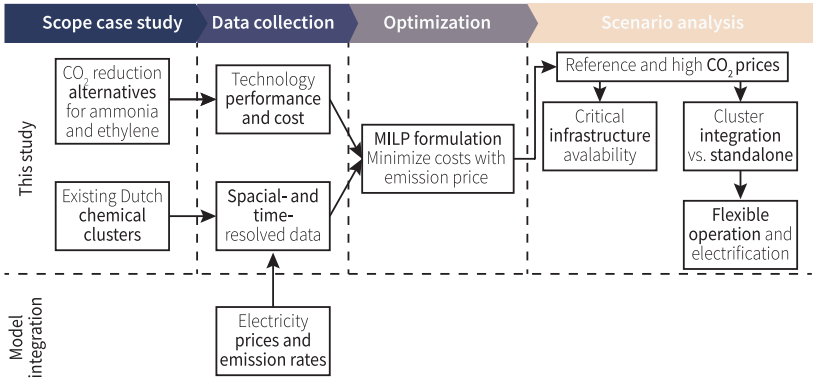

Figure 1. Block diagram illustrating the methodological steps employed in this study.

Table 1. Annual Production Capacities of Ammonia and Ethylene and the Downstream Energy and Product Demand for the Chemelot and Zeeland Cluster[a]

node	ammonia production [kt/y]	ethylene production [kt/y]	CO_2 utilization [kt/y]	downstream steam consumption [TJ/y]	downstream electricity consumption [TJ/y]	downstream fuel gas consumption [TJ/y]
Chemelot	1184	1310	383	877	2724	218
Zeeland	1819	1825	901	17242	2940	–

[a]Please note that the energy required to produce ammonia and olefins is excluded from this table.

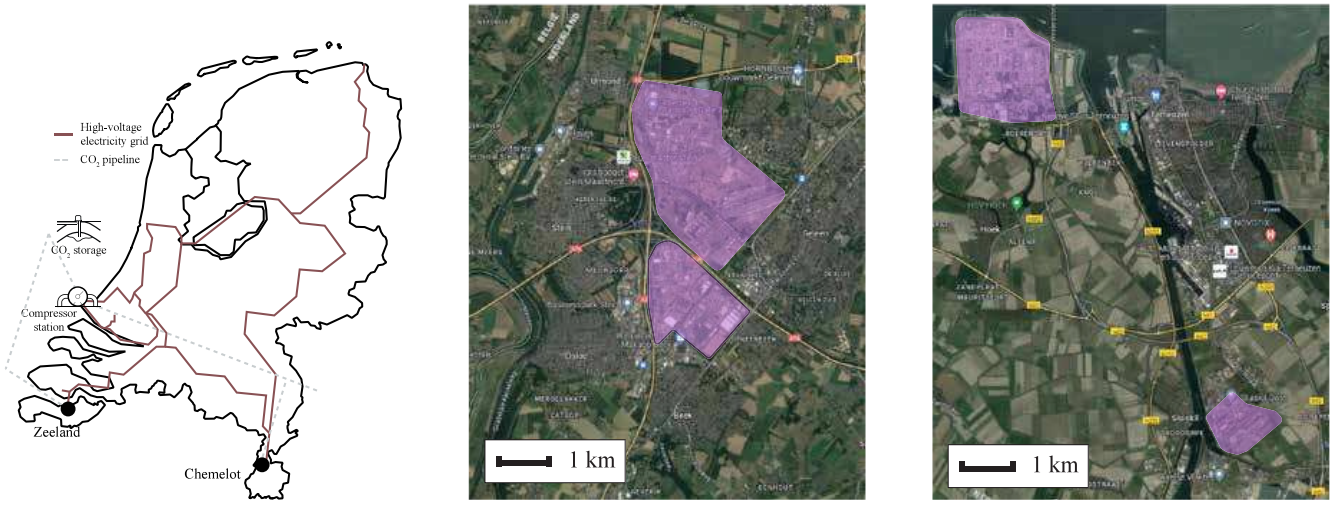

(a) Netherlands (b) Chemelot (c) Zeeland

Figure 2. (a) Map of The Netherlands, indicating the geographical locations of the Chemelot and Zeeland clusters, as well as the CO_2 transport routes, compression station, and storage site. The intercluster distance is 158 km, and the distance from Chemelot to the harbor is 230 km. (b, c) Satellite images of the Chemelot clusters (panel (b)) and the Zeeland clusters (panel (c)), with industrial areas highlighted in purple. Chemelot covers 8.0 km^2 and Zeeland covers 5.1 km^2.

■ EMISSION REDUCTION IN CHEMICAL CLUSTERS

Figure 1 outlines the methodological steps and scenarios used to evaluate emission reduction in integrated industrial clusters. The study begins by scoping the work, selecting existing Dutch chemical clusters as case studies, and identifying alternative emission reduction technologies. Cost, performance, and spatially and temporally resolved cluster data (e.g., energy and feedstock prices) are then collected as inputs for formulating an MILP model, detailed in the following chapter. The results analyze the optimal cluster design and operation under varying emission price scenarios, while assessing the impact of critical infrastructure development and process integration. Finally, the flexibility potential of electrified processes is assessed.

The chemical clusters studied in this work, Chemelot and Zeeland, are two of the four main chemical clusters found in The Netherlands; both produce ammonia and ethylene as their main products, but at different annual volumes and with varying downstream processes. Table 1 shows the associated annual production capacities of ammonia and ethylene along with the downstream consumption of CO_2, steam, electricity, and fuel gas. The total energy consumption associated with the production of ammonia and ethylene, excluding downstream processes, is estimated at 71.6 PJ/year for Chemelot and 111.4 PJ/year for Zeeland.[21−23] Because of the differences in production scale, the ammonia-to-ethylene ratio, and the nature of downstream processes, distinct challenges characterize the endeavor of reducing emissions at the two sites.

https://doi.org/10.1021/acs.iecr.4c03817
Ind. Eng. Chem. Res. 2025, 64, 4479−4497

Furthermore, the different geographical locations of the Chemelot and Zeeland clusters, which are shown in Figure 2a, result in different accesses to critical infrastructures. This disparity is reflected in their electricity prices, grid connection capacities, and CO_2 transport costs and capacities. Additionally, Figures 2b and 2c illustrate variations in the available area and plant distribution, which can influence the cluster expansion and the intracluster infrastructure and integration. The model we develop here incorporates the features of the clusters' critical infrastructure, annual production volumes, and downstream energy demands as exogenous input parameters. Notably, both clusters are also subject to a CO_2 emission price,[24] and energy and feedstock can be purchased at fixed prices. By varying these parameters, we can assess their impact on the optimal emission reduction strategies.

Emission Reduction Routes. At a cluster level, we consider three emission reduction routes: (1) amine-based carbon capture from flue gases, (2) electrification of heat provision (e.g., via electric crackers, reformers, and boilers), and (3) hydrogen production with electrolyzers. Moreover, these are complemented by electricity and material storage. The choice of these technology options among the several possibilities is consistent with a short/medium-term perspective; in other words, these technologies are either commercially available (e.g., electrolyzers, carbon capture) or close to full-scale deployment (electric crackers and reformers). The resulting optimal reduction configurations are compared to the baseline ethylene and ammonia production processes. Figure 3 provides an overview of the available production processes and technologies at the cluster level, which is valid for both Chemelot and Zeeland; the figure also shows the interactions with the downstream processes and the surrounding infrastructure. In the following, we discuss the main aspects of the different technologies; for a detailed description of the technology cost and performance parameters, the reader is referred to the Supporting Information (SI).

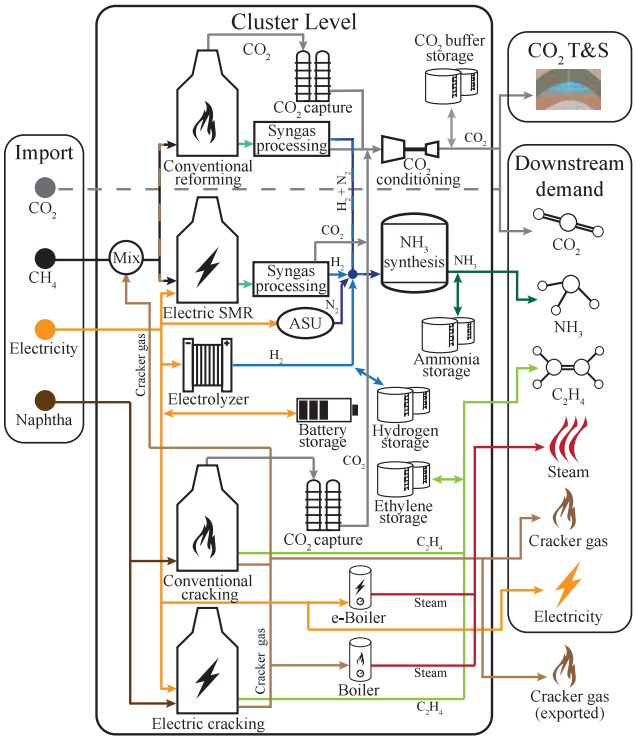

Figure 3. Overview of the processes and technologies available at the cluster level for Chemelot and Zeeland. Syngas processing includes the water gas shift (WGS) reaction and the CO_2 separation. The left side of the figure displays energy carriers and feedstocks supplied by the surrounding infrastructure, while the right side shows downstream demands and options for CO_2 and cracker gas export. CO_2 is included to enable low-CO_2 ammonia and ethylene production processes while meeting downstream demand.

Baseline Production. Ethylene and other light olefins are traditionally produced by steam cracking of hydrocarbon feedstocks, typically naphtha in Europe and Asia, and ethane in North America and the Middle East.[25] In this work, we use a naphtha cracking plant as the baseline process for ethylene production (having Dutch clusters as an exemplary application). This plant comprises three main sections: pyrolysis, compression, and product separation. In the pyrolysis section, hydrocarbons are broken down in the cracker furnace, yielding light olefins, aromatics, hydrogen, and methane. This gaseous mixture is then purified, cooled, and compressed by using a steam-driven compressor before being separated through distillation, refrigeration, and extraction. The furnace heat is typically generated by burning cracker gas, a byproduct consisting of methane and ~11% hydrogen, which reduces the need for additional energy beyond the naphtha feedstock. We assume that the cracker gas can be used as a fuel or feedstock only in those processes where hydrogen is allowed. To balance the plant's heat requirements, additional steam can be generated using a gas-fired or electric boiler, with the gas boiler fueled by either pure methane or cracker gas.

Conventional ammonia production involves two energy-intensive reforming steps and one WGS step to generate hydrogen from fossil-based feedstock. Traditionally, pure methane serves as the primary fuel and feedstock; however, in this study, we explore the feasibility of utilizing cracker gas as an alternative. The process starts with desulfurization and prereforming, after which the steam-feedstock mixture (ratio 2.7) enters the steam methane reforming (SMR) step, where fuel combustion provides the necessary heat for the endothermic reaction. In the following autothermal reforming (ATR) step, the feedstock reacts with compressed air, increasing the hydrogen yield and supplying the nitrogen needed for ammonia synthesis. The resulting syngas is then cooled, water is extracted, and a two-step adiabatic WGS maximizes hydrogen production. After the WGS, ~99% of the CO_2 is removed from the syngas via methyldiethanolamine (MDEA) absorption, producing a pure CO_2 stream, which is then compressed to 150 bar for utilization or storage. Any remaining CO and CO_2 are converted to methane in a methanation reactor. A cryogenic purification unit adjusts the hydrogen-to-nitrogen ratio in the reactor effluent to the stoichiometric requirement for the Haber Bosch (HB) process, where ammonia is synthesized under high temperature and pressure (150 bar). The waste stream, containing impurities (methane and argon) along with excess nitrogen and hydrogen, is recycled as fuel for the primary reformer and the ATR air compressor gas turbine.

The conventional ammonia production process maximizes heat integration by utilizing exhaust heat from air compression in the primary reformer's furnace and recovering heat from the ATR exit. Additionally, the exothermic WGS and HB reactions generate heat, producing high-pressure superheated steam, which is used for electricity generation, for the reforming reaction, and to supply heat in the CO_2 reboiler. As near/medium-term future ammonia production is still expected to

https://doi.org/10.1021/acs.iecr.4c03817
Ind. Eng. Chem. Res. 2025, 64, 4479−4497

rely on the HB process, we separate the reforming and ammonia synthesis sections, accounting for their respective energy consumption and production, and evaluate more sustainable alternatives for the syngas production step.

Ammonia and ethylene are key platform chemicals for various downstream products. Since the production processes for these downstream chemicals are expected to remain unchanged in the near future, they are not explicitly modeled in this analysis. However, their energy and material consumption are included as the downstream demand. A detailed list of these downstream processes and their energy consumption is provided in the Supporting Information (SI).

Carbon Capture from Flue Gas. Naphtha cracking and SMR are endothermic processes that generate CO_2 through fuel combustion for the provision of reaction energy. We consider capturing these CO_2 emissions from the resulting flue gas using a state-of-the-art CC process utilizing monoethanolamine (MEA) solvent for both the cracker furnace and the SMR.[26] The fuel used for combustion can be natural gas or a combination of natural gas and cracker gas, yielding a maximum hydrogen share of 11%. Consequently, the CO_2 molar fraction in the flue gas ranges between 6.2% and 9.5%.

In ethylene production, all direct emissions come from heat production. In ammonia production, ∼30% of emissions come from the reformer flue gas, while the remaining 70% arises from CO_2 in the syngas. The latter only needs compression before CO_2 utilization or storage. Thus, flue gas CC in ammonia production requires a capture plant smaller than that in the case of ethylene, reducing specific costs and energy consumption. However, the total CO_2 production per tonne product is higher for ammonia than for ethylene, which affects the feasibility of the CC route, as it depends on the availability of sufficient CO_2 transport and storage infrastructure.

Electrification of Heat Production. Another approach for reducing direct emissions from heat production in chemical processes is to replace fuel-fired furnaces and boilers with electric ones. In the electric naphtha cracking plant, the conventional furnace is replaced by an electric furnace, and steam compressors are substituted with electric compressors, while the rest of the plant remains substantially unchanged.[27] In electric ammonia production, syngas is produced using electric steam methane reforming (eSMR) that replaces conventional SMR, while the ATR is removed from the process. Therefore, for ammonia synthesis, nitrogen must be produced separately by an air separation unit (ASU).

While electrifying low-temperature heat is often discussed in the context of industrial decarbonization, electrifying high-temperature heat presents additional challenges. However, ongoing research is exploring technologies such as electric resistance heating for cracking and reforming to address these challenges.[28−30] Configurations using electric resistance heating offer several advantages, including improved thermal efficiency, greater flexibility, scalability, and typically smaller size.[29] Consequently, these configurations demonstrate superior energetic performance and can lead to reduced investment costs.

Although electrification eliminates direct process emissions, its effectiveness depends on the carbon intensity of the electricity used and the lifecycle emissions of the products. For ammonia production, it is crucial that separated process-related CO_2 is not emitted. In ethylene production, byproducts, particularly the increased cracker gas yield, should not be combusted elsewhere to produce electricity or heat. Therefore, we assign the combustion corresponding to the CO_2 emission to the export of cracker gas. Furthermore, it should be noted that lifecycle emissions of products for both industries could be eliminated by switching to alternative biobased or synthetic feedstocks.

Hydrogen Production with Electrolyzers. While the adoption of CC or electrification can reduce up to 99% of direct process emissions in the ammonia industry, it does not eliminate the need for carbon feedstocks or the production of CO_2. Additionally, energy is required to separate the CO_2, and substantial infrastructure is needed for its transport and storage. Electrolyzers present a promising alternative by producing carbon-free hydrogen through water electrolysis without generating CO_2. However, they require significantly more low-carbon electricity, over five times more per tonne of ammonia, compared to eSMR.

Similar to hydrogen production via eSMR, the electrolyzer route requires an ASU to produce nitrogen for the ammonia synthesis. In this work, we consider an alkaline electrolysis cell (AEC) as an electrolysis technology due to its relatively low capital expenditures (CAPEX) and higher maturity, compared to other electrolyzer technologies. Although other types may have slightly better energy and dynamic performance, these differences are negligible within our analysis's temporal resolution and scope.

Dynamic Operation and Storage. The dependency of electrification routes on low-carbon electricity, combined with the variability of renewable sources, presents challenges for integrating these processes following a classical 24/7 operational approach. While conventional chemical processes typically operate at full load due to significant capital investment and process complexity, volatile electricity prices, high shares of renewable electricity, and grid congestion risks may call for dynamically operated industrial processes (despite the higher initial capital investment).

While the dynamic operation of electric cracking and SMR has not been proven commercially, research indicates that electrified reactors offer significantly greater flexibility compared to conventional reactors.[29,30] For example, recent work by From et al.[28] demonstrated that a pilot-scale eSMR reactor can transition from an idle state at 645 °C to full-load operating conditions at 900 °C with a rate of 120 °C/h. The analysis of the operation envelope (OE) shows a minimum operating temperature of 750 °C, achievable within 1 h from idle, and a power load range (representing the OE) of 60% of the capacity. The ramping time (RT) from idle to maximum capacity is 2.5 h. Therefore, in this work, we assume similar dynamics for the electric naphtha cracker reactor, adopting the same OE and RT. This was also confirmed by Armijo and Philibert,[31] who additionally found an RT of 5 h and an OE between 40% and 100% for the ASU and HB plant.

The dynamic operation parameters for all technologies are summarized in Table 2, categorized as slow, medium, and fast. As slow conventional technologies lack dynamic operation data, we assume a conservative OE of 5%−10% and an RT four times slower than the electric alternative. Slow technologies are assumed to operate continuously without the ability to shut down or start up. Medium-dynamic technologies can temporarily shut down production but maintain their reactors at a warm idle state, consuming a fraction of the plant's maximum load at reference capacity, referred to as the warm standby power (WSP). Fast technologies operate without limitations.

Dynamic operation requires larger installed plant capacities to meet the same annual demand. For the electric plants and the

https://doi.org/10.1021/acs.iecr.4c03817
Ind. Eng. Chem. Res. 2025, 64, 4479−4497

Table 2. Dynamic Operation Parameters of the Considered Technologies

	dynamics type	OE [%]	RT [h]	WSP [%]
conventional steam cracker	slow	5	10	–
conventional steam cracker with CC	slow	5	10	–
electric steam cracker	medium	60	2.5	5
conventional reformer	slow	10	10	–
conventional reformer with CC	slow	10	10	–
electric reformer	medium	60	2.5	5
alkaline electrolyzer	medium	80	<1	5
Haber Bosch process	medium	70	5	0
gas-fired boiler	fast	100	<1	–
electric boiler	fast	100	<1	–
air separation unit	medium	70	5	0

electrolyzer, we assume a maximum capacity of twice that of their currently installed capacity, which is different for both clusters. Conventional and CC technologies are constrained to their current installed capacities, as dynamic operation is neither technically feasible nor economically viable for these technologies.

To accommodate for the dynamic operation of key reactors under the assumption of inflexible and constant downstream processes and demand, five types of material and energy storage technologies have been incorporated into this study: ethylene tank, ammonia tank, CO_2 buffer tank, hydrogen tank, and a Li-ion electricity battery. A detailed description of the types of storage and the associated costs and performance data can be found in the SI.

Existing chemical clusters, especially in semiurban environments like in The Netherlands, have limited land available for new technologies. Of course, the exact amount of extra land available is uncertain and dependent on the specific characteristics of the sites. As this information is not publicly available, we assume that each of the five storage technologies can occupy up to 2% of the total area of the clusters, amounting to an additional 10% of land compared to the original size. For Chemelot, this equates to 160 000 m^2, while for Zeeland 101 400 m^2. The maximum capacity for battery storage is calculated based on the energy density of Tesla's Megapack.[32] For tank storage, we assume that a maximum of 50% of the available additional area can used for storage, with the remaining 50% required as buffer and piping space. Assuming a tank height of 4 m, we calculate the maximum storage capacity based on the densities at storage conditions. As for batteries, since the maximum charge and discharge capacities are more dependent on the grid connection rather than on the battery size, we use a size-independent capacity equivalent to that of a large-scale DC cable, such as a 700 MW offshore wind connection.[33] For storage tanks, we assume charging and discharging capacities equal to the maximum expected production of the clusters, which is twice that of a typical full-scale plant.

Cluster Input Data. *Critical Infrastructure and Feedstock Prices.* Apart from technology performance, our model requires time- and space-discretized information. While weather data are rather straightforward, as they have been provided by the national weather institutions for several past years (in our case, KNMI), electricity prices and CO_2 intensity profiles are particularly challenging: they depend—to name a few—on the future electricity system, demand, and grid configuration. Therefore, we adopted data as predicted for 2030 by a comprehensive hourly resolved electricity system model developed by the Dutch Organization for Applied Scientific Research (TNO).[34] Notably, the model incorporates nodal pricing to reflect grid congestion and uses as input the prediction of the IP2024 Klimaat Ambities for 2030[35] and the 2020 TYNDP Global Ambitions[36] scenarios. Figure 4 illustrates the resulting electricity price profiles and distributions for Chemelot and Zeeland as well as the grid emissions profile. We can observe that electricity prices in Zeeland are generally lower than in Chemelot due to reduced grid congestion, with prices reaching zero ∼20% of the time.

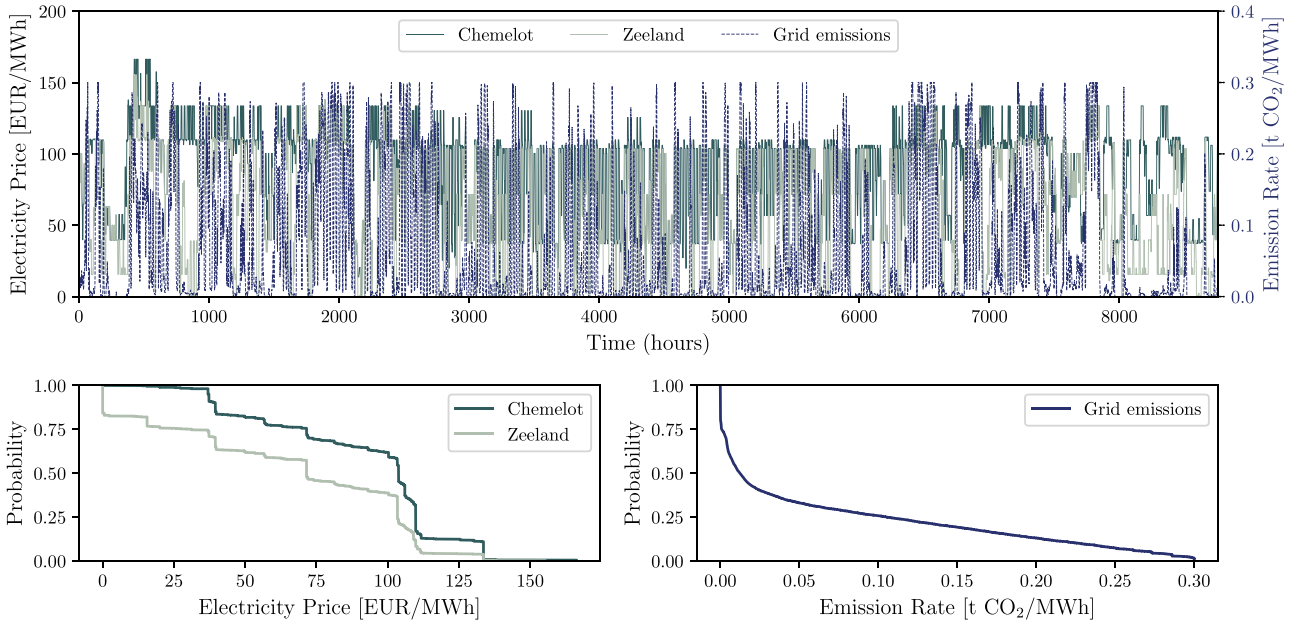

Figure 4. Hourly electricity prices and grid emissions (top figure) and their respective cumulative distributions (bottom two figures) for Zeeland and Chemelot.

https://doi.org/10.1021/acs.iecr.4c03817
Ind. Eng. Chem. Res. 2025, 64, 4479−4497

Table 3. Costs and Capacities of Critical Infrastructure for the Two Chemical Clusters, Including the CO_2 Transport and Storage Costs and Capacities, Grid Capacities, Feedstock Prices, and CO_2 Emission Prices[a]

node	industry area [km^2]	CO_2 storage cost [€/tCO_2]	CO_2 transport capacity [t/h]	grid connection capacity [MW]	methane price [€/MWh]	naphtha price [€/t]	CO_2 emission price [€/t]
Chemelot	8.00	62.7	115 (115−285)	2000 (650−2000)	100	732	150.31 (150.31−250)
Zeeland	5.07	54.6	171 (171−285)	3000 (650−3000)	100	732	150.31 (150.31−250)

[a]The values in brackets indicate the range of parameters studied.

Table 4. Performance and Cost Parameters of the Conventional Processes and the Respective Alternative CC and Electrification Routes[a]

process	inputs	input ratio, $\beta_{m,n''}$	outputs	output ratio, $\alpha_{m,n'}$	emission factor, κ_m [t/input]	source
conventional steam cracker	{naphtha, steam, electricity}	[1, 0.082, 0.083]	{ethylene, cracker gas}	[0.303, 0.781]	0.327	27
conventional steam cracker with CC	{naphtha, steam, electricity}	[1, 0.402, 0.107]	{ethylene, cracker gas, CO_2}	[0.303, 0.781, 0.295]	0.033	27
electric steam cracker	{naphtha, electricity}	[1, 1.942]	{ethylene, cracker gas, steam}	[0.303, 2.649, 0.050]	–	27
conventional reformer	{gas,[b] steam}	[1, 0.087]	{hydrogen, CO_2, electricity, nitrogen}	[0.761, 0.112, 0.024, 0.154]	0.067	45
conventional reformer with CC	{gas,[b] steam}	[1, 0.087]	{hydrogen, CO_2, electricity, nitrogen}	[0.761, 0.112, 0.007, 0.215]	0.007	45
eSMR	{gas,[b] electricity}	[1, 0.272]	{hydrogen, CO_2}	[0.927, 0.201]	0.003	46
AEC	{electricity}	[1]	{hydrogen, heat low T, oxygen}	[0.629, 0.163, 0.149]	–	47
HB process	{hydrogen, nitrogen, electricity}	[1, 0.139, 0.056]	{ammonia, steam}	[0.168, 0.114]	–	47
ASU	{electricity}	[1]	{nitrogen, oxygen}	[4.000, 1.227]	–	47
gas-fired boiler	{gas[b]}	[1]	{steam}	[0.920]	0.203	27
electric boiler	{electricity}	[1]	{steam}	[0.990]	–	27

process	unit	Chemelot S_m^{max}	Zeeland S_m^{max}	size-based CAPEX, λ_m [$kEUR_{2022}$/unit]	size-independent CAPEX, ζ_m [$MEUR_{2022}$]	maintenance costs (ψ) [%]	lifetime [yr]	source
conventional steam cracker	t naphtha/h	521	815	2083	543	4.0	25	27
conventional steam cracker with CC	t naphtha/h	521	815	2728	558	4.0	25	26, 27
electric steam cracker	t naphtha/h	1042	1630	2083	543	4.0	25	27
conventional reformer	MW_{gas}	1269	1949	574	170	3.8	25	48
conventional reformer with CC	MW_{gas}	1269	1949	671	185	3.8	25	26, 48
eSMR	MW_{gas}	1736	2667	525	127	3.9	25	46
AEC	MW_e	2558	3930	684	–	2.0	19	47
HB process	MW_{H2}	1609	2472	439	105	3.8	25	48
ASU	MW_e	56	86	4224	25	4.2	25	49
gas-fired boiler	MW_{th}	550	1100	106	–	4.0	25	27
electric boiler	MW_e	550	1100	154	–	1.0	25	27

[a]All CAPEX values represent the total plant costs and are adjusted to 2022 by using the chemical engineering plant cost index (CEPCI). [b]The gas for the reformer process, the eSMR, and the gas-fired boiler can be a mixture of methane and cracker gas.

We set the anticipated grid capacities from the clusters' energy strategies as the upper limit for electricity imports.[37,38] As for other relevant feedstock and energy imports, we use an average 2022 naphtha price of 732 €/tonne[39] and a projected methane price of 100 €/tonne[40] for both clusters. Additionally, we account for the transport and storage costs of CO_2 to the Dutch Porthos offshore storage project, which connects the clusters to the Rotterdam harbor[41] and subsequent offshore storage. For Chemelot, we increase the costs by 15% to account for onshore pipeline routes, while assuming a direct offshore CO_2 pipeline from Zeeland to the storage site. Given that the Porthos storage project has an expected capacity of 2.5 million tonnes per year, we assume a 1 million tonne per year onshore pipeline for Chemelot and a 1.5 million tonne per year offshore pipeline for Zeeland. While this assumption is optimistic—implying exclusive access to the storage capacity for these two clusters—we assess the impact of varying access to CO_2 transport and storage. Additionally, we use a CO_2 emission price of €150.31, the minimum price for 2030 as set by the Dutch Emissions Authority (NEA).[24] Considering the possibility of a higher ETS price, we also include a scenario with a CO_2 emission price of €250, which is a more realistic level to incentivize deeper decarbonization. Table 3 summarizes the cluster-specific data.

Downstream Processes. The annual production volumes of ammonia, ethylene, and other chemicals produced in both clusters are based on the capacities reported in Eerens and Dam,[22] Batool and Wetzels,[21] Oliveira and Dril.[23] The downstream processes are represented in the model by their CO_2 and energy demands. Table S1 in the SI includes a more-detailed list of products and energy consumptions from downstream processes for both clusters, while Table 1 shows the resulting production capacities and downstream energy and

https://doi.org/10.1021/acs.iecr.4c03817
Ind. Eng. Chem. Res. 2025, 64, 4479−4497

Table 5. Cost and Performance Parameters of Energy and Material Storage Technologies

	unit	charge efficiency, η^C [%]	discharge efficiency, η^D [%]	electricity consumption [MWh/t]	storage density [unit/m^3]	Chemelot storage capacity [unit]	Zeeland storage capacity [unit]	maximum charge/discharge rate [unit/h]
ethylene tank	t ethylene	100	100	–	0.566	181312	114906	250
ammonia tank	t ammonia	100	100	–	0.681	218000	138158	250
CO_2 buffer tank	t CO_2	100	100	0.045	1.156	369824	234376	650
hydrogen tank	MWh	100	100	–	0.417	133565	24324	1500
Li-ion battery	MWh	98	97	–	0.040[a]	6414	4065	700

	unit	CAPEX λ_m [k€$_{2022}$/unit]	maintenance costs (ψ) [%]	lifetime [y]	source
ethylene tank	t ethylene	26.2	2.0	25	27
ammonia tank	t ammonia	8.7	3.0	25	47, 50
CO_2 buffer tank	t CO_2	1.0	6.0	25	50, 51
hydrogen tank	MWh	32.2	1.1	25	52
Li-ion battery	MWh	228.5	1.5	20	53

[a]The storage density of the battery is in MWh/m^2.

material demands. Given that downstream processes in the fertilizer and high-value chemicals industry typically maintain a constant operational level, these volumes are treated as exogenous fixed hourly demands.

PROBLEM FORMULATION

Modeling Framework. The optimization framework adopted in this research builds upon a well-established, open access MILP modeling framework outlined in the work of Wiegner et al.[42] Its flexible temporal, spatial, and technological resolution enables it to address a variety of optimization problems in the realm of energy and chemical technologies. Here, we employ a one-year hourly resolution for the two clusters.

Several of the cost and performance models used in this work are based on the cracker model formulated in Tiggeloven et al.,[27] which were adapted for a cluster case study. To incorporate the spatial representation of individual industry clusters, we adopt the energy hub methodology proposed by Geidl et al.[43] Following this methodology, we treat each industry cluster as an energy hub that can facilitate the conversion or storage of considered materials and energy carriers through a range of technologies and industrial processes. Each energy hub includes import and export limits, prices, and demands. Furthermore, the model can facilitate interhub transportation of material and energy carriers. The framework optimizes decision variables simultaneously including design variables (e.g., process or technology selection and sizing) and operational variables (e.g., energy/material flows and storage levels). The general formulation of the MILP is

$$\min_{\mathbf{v},\mathbf{w}} f(v, w) \tag{1}$$

subject to

$$\mathbf{A}v + \mathbf{B}w = \mathbf{b}$$
$$v \geq 0 \in \mathbb{R}^{N_v},\ w \in \{0, 1\}^{N_w}$$

where f is the objective function with v and w as the continuous and binary decision variables, respectively. The matrices $\mathbf{A}$ and $\mathbf{B}$ denote the corresponding constraints, with $\mathbf{b}$ as the known term of the constraint, and N indicating the dimensionality of v and w. The problem is solved using Gurobi v11.0.[44]

Objective Functions. Two different objective functions can be minimized: total costs and net CO_2 emissions. Similar to our previous work,[27] the total cost of the optimized system is represented by the sum of the capital and operational expenditures of the system; the latter is divided into the import costs of material and energy carriers, the expenses associated with CO_2 transport and storage, and the CO_2 emission price:

$$C = C^{\text{CAPEX}} + C^{\text{import}} + C^{\text{CO}_2\text{ storage}} + C^{\text{CO}_2\text{ emission}} \tag{2}$$

where the annualized technology cost is defined as

$$C^{\text{CAPEX}} = \sum_{h\in\mathcal{H}} \sum_{m\in\mathcal{M}} (1 + \psi_m)(\lambda_m S_{m,h} + \zeta_m)\omega_m \tag{3}$$

Here, $\mathcal{M}$ denotes the set of installed technologies and $\mathcal{H}$ the set of industry clusters, $S_{m,h}$ is the decision variable for the size of technology m in cluster h, λ_m and ζ_m represent the size-dependent and size-independent cost parameters, and the annuity factor ω_m is utilized to calculate the annualized capital costs. The fixed maintenance cost of the technology is incorporated as a fraction of the annual capital costs, denoted by ψ_m. The cost parameters of all industrial processes and storage technologies are listed in Tables 4 and 5, respectively. The import costs include the expenses associated with material and energy carriers that cannot be produced within the system boundaries of the model, such as electricity, methane, and naphtha, and are consequently bought at market price. These costs are calculated as

$$C^{\text{import}} = \sum_{h\in\mathcal{H}} \sum_{n\in\mathcal{N}} \sum_{t=1}^{T} (\iota_{n,t,h} I_{n,t,h}) \tag{4}$$

where $\mathcal{N}$ is the set of carriers and T is the set of timesteps, $I_{n,t,h}$ is the amount of imported carrier and $\iota_{n,t,h}$ the hourly carrier price at hour t and cluster h. We assume constant naphtha and methane prices for the full time horizon and all clusters, while the electricity prices vary per cluster and time step, as described in the previous section. We calculate the CO_2 transport and storage costs as

https://doi.org/10.1021/acs.iecr.4c03817
Ind. Eng. Chem. Res. 2025, 64, 4479−4497

$$C^{\mathrm{CO_2\ storage}} = \sum_{h\in\mathcal{H}}\sum_{t=1}^{T}(\nu_{\mathrm{CO_2},h}J_{\mathrm{CO_2},t,h}) \tag{5}$$

where $J_{\mathrm{CO_2},t,h}$ is the amount of CO_2 export and stored, and $\nu_{\mathrm{CO_2},h}$ is the costs per tonne of CO_2 transported to storage.

The total CO_2 emissions are calculated by summing the direct technology emissions and the indirect emissions from imported electricity, as follows:

$$E = \sum_{h\in\mathcal{H}}\sum_{t=1}^{T}\sum_{m\in\mathcal{M}}(\kappa_m F_{m,n_{\mathrm{main}},t,h} + \varepsilon_{\mathrm{electricity},t,h}I_{\mathrm{electricity},t,h}) \tag{6}$$

where $F_{n_{\mathrm{main}},m,t,h}$ represents the consumption of the main input carrier n_{main} of technology m, κ_m is the emission factor of the technology, and $\varepsilon_{\mathrm{electricity},t}$ is the hourly CO_2 emission factor of the electricity grid. The expenses related to the CO_2 emission price are calculated as

$$C^{\mathrm{CO_2\ emission\ price}} = \theta E \tag{7}$$

where θ is the CO_2 emission price for the system. By including (multiple) CO_2 emission prices, we can further explore the interaction between cost minimization and emissions without resorting to a computationally heavy multiobjective optimization approach (we note that the emission minimization points took 40−90 h). Note that, when minimizing emissions, the total cost C is replaced by the total CO_2 emissions E as the objective function.

Constraints. *Energy and Material Balance.* Energy and material balances are added for each cluster h as equality constraints for each carrier n and each hour t, and are formulated as follows:

$$\sum_{m\in\mathcal{M}}(P_{m,n,t,h} - F_{m,n,t,h}) + I_{n,t,h} - J_{n,t,h} - D_{n,t,h} = 0 \tag{8}$$

where $P_{m,n,t,h}$ and $F_{m,n,t,h}$ are the input and output of technology m, $I_{n,t,h}$ and $J_{n,t,h}$ are import and export to/from each cluster h from/to outside the system boundaries and $D_{n,t,h}$ is the demand.

Performance of Industrial Processes. Each industrial process is treated as an input/output conversion technology with a specific conversion efficiency. The material and energy conversion efficiency of chemical processes depends on several factors, including the plant design capacity, the specific operation mode (on-design vs off-design), and the dynamic operation (transient vs steady-state phase). For example, during part-load operation, chemical processes typically have reduced conversion efficiency and increased energy consumption per unit of product. While similar behaviors can be modeled via piecewise functions, this would introduce several new integer variables adding significant additional complexity. Considering also the lack of reliable part-load performance data for the considered processes, we decided to model chemical processes with a linear approximation of the conversion performance and constant conversion efficiency across both part-load and full-load operations. Therefore, the industrial processes feature the same formulation of the conversion performance constraints with variations in their dynamic operation modeling.

The general conversion constraints are based on the electric cracker model formulation reported in Tiggeloven et al.[27] and are adapted to suit generic chemical processes. The performance parameters of all conversion technologies and processes are listed in Table 4. The process production P and consumption F are calculated as

$$P_{m,n',t,h} = \alpha_{m,n'}F_{m,n_{\mathrm{main}},t,h} \tag{9}$$

and

$$F_{m,n'',t,h} = \beta_{m,n''}F_{m,n_{\mathrm{main}},t,h} \tag{10}$$

where $\alpha_{m,n'}$ and $\beta_{m,n''}$ denote the conversion efficiency per unit of input for outputs $n' \in \mathcal{N}' \subset \mathcal{N}$ and the ratio between inputs $n'' \in \mathcal{N}'' \subset \mathcal{N}$, respectively.

Moreover, the capacity of all conversion and storage technologies is constrained by

$$S_m^{\min} \le S_{m,h} \le S_m^{\max} \tag{11}$$

where $S_{m,h}$ is the installed capacity of technology m at cluster h, and $S_m^{\min}$ and $S_m^{\max}$ are the minimum and maximum capacity of technology m, respectively.

The operation envelope OE of a process is determined by the minimum load point and is constrained by the following:

$$\gamma_{m,n_{\mathrm{main}}}x_{m,t,h}S_{m,h} \le F_{m,n_{\mathrm{main}},t,h} \le x_{m,t,h}S_{m,h} \tag{12}$$

where $x_{m,t,h} \in \{0, 1\}$ represents the on/off status of the technology and $\gamma_{m,n_{\mathrm{main}}}$ is the minimum feasible operating point of the technology as a fraction of the installed capacity, $S_{m,h}$. It is worth noting that both $x_{m,t,h}$ and $S_{m,h}$ are decision variables, which introduce bilinearity into this constraint and require the inclusion of an auxiliary big-M constraint to resolve it.

To account for the ramping behavior of processes, we introduce the following inequality constraint:

$$-\frac{S_{m,h}}{RT} \le F_{m,n_{\mathrm{main}},t,h} - F_{m,n_{\mathrm{main}},t-1,h} \le \frac{S_{m,h}}{RT} \tag{13}$$

Here, RT denotes the time needed to ramp up or down between the idle state and the installed capacity $S_{m,h}$. This constraint suggests that by increasing the installed capacity of a plant it can achieve a greater maximum load change rate $\frac{S_{m,h}}{RT}$. Since the rate of temperature change is often independent of the reactor size, we assume that the RT term also remains constant for reactor sizes other than the reference size.

Given the diversity of processes and conversion technologies present in chemical clusters, we distinguish between three categories: (1) slow technologies, (2) medium-dynamic technologies, and (3) fast technologies. While all three categories of technologies follow the constraints described above, we have additional considerations per type:

- **Slow technologies:** Conventional production processes typically fall into the category of slow technologies, characterized by small OEs, slow ramping behavior, and extended start-up and shut-down times of up to 24 h or more. To accommodate this, we linearize eq 12 by excluding $x_{m,t,h}$ for these technologies (implying no startups and shutdowns), allowing for operation within their OE only.
- **Medium-dynamic technologies:** Medium-dynamic technologies typically have an OE exceeding 50% and allow for startups and shutdowns of the production, while maintaining the process at a warm standby by consuming electricity. Depending on the technology, the ramping behavior may be constrained. It is worth noting that, for these technologies, we assume that the maximum load

https://doi.org/10.1021/acs.iecr.4c03817
Ind. Eng. Chem. Res. 2025, 64, 4479−4497

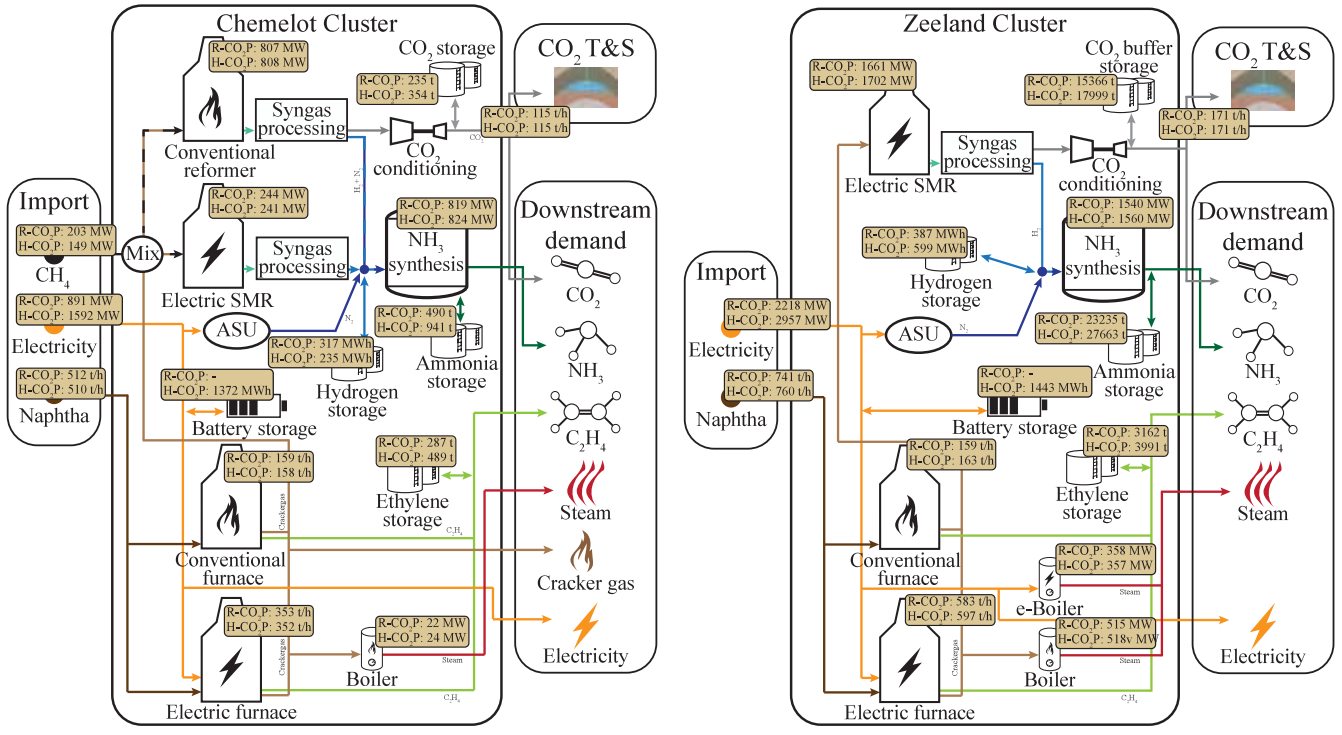

Figure 5. Optimal selection and sizes of technologies and maximum import/export in the (a) Chemelot and (b) Zeeland cluster for the reference (R-CO_2P: 150.31 €/t CO_2) and high (H−CO_2P: 250 €/t CO_2) emission price scenarios. Syngas processing includes the WGS reaction and the CO_2 separation.

change rate $\frac{S_{m,h}}{RT}$ is greater than or equal to the minimum operating point $\lambda_m S_{m,h}$ to ensure that the technology can go from idle to the minimum operation state within 1 h. Additionally, we introduce a constraint to account for warm standby:

$$F_{m',\text{electricity},t,h} \geq (1 - x_{m',t,h})\phi_{m'} S^{\text{ref}}_{m',h} \tag{14}$$

Here, $\phi_{m'}$ represents the WSP as a fraction of the maximum electric power of the reference size $S^{\text{ref}}_{m',h}$ of medium-dynamic technology $m' \in \mathcal{M}' \subset \mathcal{M}$. Consequently, the equality sign in eq 10 is replaced by an inequality sign.

- **Fast technologies:** With an OE of 100% and unconstrained ramping behavior, fast technologies can operate without ramping limitations in an hour. Hence, we linearized eq 12 by excluding $x_{m,t,h}$ while eq 13 is dropped.

Performance of Storage Technologies. The storage technologies incorporate storage level $L_{m'',t,h}$ as an additional decision variable in their performance model, subject to the following constraint:

$$0 \leq L_{m'',t,h} \leq S_{m'',h} \tag{15}$$

Here, $\mathcal{M}''$ represents a subset of storage technologies within the broader technology set $\mathcal{M}$. Furthermore, the charging and discharging behavior is expressed as

$$L_{m'',t,h} = L_{m'',t-1,h} + F_{m'',t,h}\eta^{C}_{m''} - \frac{P_{m'',t,h}}{\eta^{D}_{m''}} \tag{16}$$

where $\eta^{C}_{m''}$ and $\eta^{D}_{m''}$ represent the charging and discharging efficiencies of storage technology m''. To avoid simultaneous charging and discharging, a binary variable is introduced in the maximum charging and discharging constraints:

$$F_{m'',t,h} \leq S^{\text{charge max}}_{m''} g_{m'',t,h} \tag{17}$$

and

$$P_{m'',t,h} \leq S^{\text{discharge max}}_{m''}(1 - g_{m'',t,h}) \tag{18}$$

Here, $S^{\text{charge max}}_{m''}$ and $S^{\text{discharge max}}_{m''}$ denote the charging and discharging capacities, respectively, and $g_{m'',t,h}$ indicates whether the technology is charging ($g_{m'',t,h} = 1$) or discharging ($g_{m'',t,h} = 0$). We assume that the charging and discharging capacities are independent of the storage size. The performance parameters of all storage technologies are listed in Table 5.

Problem Complexity. The complexity of the optimization framework described above arises mainly from two variables: (1) the binary variable representing on/off status in eq 12 and (2) the binary variable representing charging/discharging in eqs 17 and 18. These operational variables are defined for each hour within the full time horizon (i.e., $T = 8760$). Additionally, for the variable $x_{m,t,h}$, auxiliary big-M constraints are required for each technology m, each time step t, and each cluster h to resolve the bilinearity in the constraint. Consequently, reducing the time resolution of the optimization problem can significantly decrease its complexity.

To reduce the time complexity, we identify a set of design days $d \in \mathcal{D}$ using the time series aggregation module (TSAM) from Kotzur and Hoffmann.[54] The TSAM is a Python package that employs various algorithms to aggregate time-dependent input data, such as weather, price, emission, and demand data, from full resolution into design day (DD)s, while preserving the hourly sequence σ of DDs. Subsequently, we apply an approach

https://doi.org/10.1021/acs.iecr.4c03817
Ind. Eng. Chem. Res. 2025, 64, 4479−4497

Table 6. Installed Capacities of the Cluster and Standalone Scenarios for Chemelot and Zeeland[a]

		Chemelot			Zeeland		
capacity	unit	optimal integrated cluster	independent ammonia synthesis	independent ethylene synthesis	optimal integrated cluster	independent ammonia synthesis	independent ethylene synthesis
Reference CO_2 Emission Price							
conventional steam cracker	tonne naphtha/h	159	–	496	159	–	688
conventional steam cracker with CC	tonne naphtha/h	0	–	0	0	–	0
electric steam cracker	tonne naphtha/h	353	–	0	583	–	0
conventional reformer	MW gas	807	0	–	0	0	–
conventional reformer with CC	MW gas	0	0	–	0	0	–
eSMR	MW feed	244	569	–	1661	899	–
AEC	MW electric	0	755	–	0	1153	–
HB process	MW hydrogen	820	938	–	1540	1428	–
ASU	MW electric	6	33	–	54	50	–
electric boiler	MW electric	0	0	0	358	0	134
gas-fired boiler	MW gas	12	0	114	515	0	537
ammonia tank	tonne	490	5038	–	23235	11131	–
Li-ion battery	MWh	0	0	0	0	0	0
CO_2 buffer storage	tonne	235	8041	0	15366	496	0
hydrogen tank	MWh	317	582	–	387	632	–
ethylene tank	tonne	287	–	0	3162	–	0
High CO_2 Emission Price							
conventional steam cracker	tonne naphtha/h	158	–	0	163	–	398
conventional steam cracker with CC	tonne naphtha/h	0	–	496	0	–	290
electric steam cracker	tonne naphtha/h	352	–	0	597	–	0
conventional reformer	MW gas	808	0	–	975	0	–
conventional reformer with CC	MW gas	0	0	–	670	0	–
eSMR	MW feed	241	552	–	1702	960	–
AEC	MW electric	0	759	–	0	1123	–
HB process	MW hydrogen	824	947	–	1560	1478	–
ASU	MW electric	6	33	–	54	51	–
electric boiler	MW electric	0	0	0	357	0	228
gas-fired boiler	MW gas	17	0	287	518	0	537
ammonia tank	tonne	941	6391	–	27663	13907	–
Li-ion battery	MWh	1372	0	277	1443	0	1152
CO_2 buffer storage	tonne	354	14801	0	17999	477	0
hydrogen tank	MWh	235	538	–	599	595	–
ethylene tank	tonne	489	–	0	3991	–	0

[a]A dashed line means that the technology is not available in the scenario.

similar to method 2 described in Gabrielli et al.[55] Since the complexity arises from technology constraints, all technologies are modeled hourly using DDs. However, the storage level is modeled at full resolution to enable the accurate representation of seasonal storage. The variables at the reduced resolution are then coupled to the full-resolution variables based on the hourly sequence σ. For more details on this method and the coupling, please refer to Gabrielli et al.[55] We found that the temporal complexity can be tackled using 20 DDs, which, as shown in the SI, allows us to maintain sufficient accuracy, compared to the full resolution while significantly reducing computation time.

As the work of Gabrielli et al.[55] does not account for constraining ramping rates of technologies, we propose an extension to their approach. This extension is necessary as the ramping constraint in eq 13 involves dependencies between time steps; i.e., the difference in input at two consecutive hours t and $t-1$ must be within a specified range. Using independent DDs for the input variable at reduced resolution would not allow for constraining the ramping at the first and the last hour of each DD. Therefore, we introduce an auxiliary input variable $F^{A}_{m,n_{\text{main}},t,h}$ at the full resolution which is used in eq 13. The rest of the technology constraints are still based on the reduced resolution input variable. The two variables are then coupled by using the following constraint:

$$F_{m,n_{\text{main}},\sigma(t),h} = F^{A}_{m,n_{\text{main}},t,h} \tag{19}$$

To reduce the complexity of the problem further, we can relax the constraints in eqs 17 and 18 by removing the binary decision variable $g_{m'',t,h}$ that indicates whether the technology is charging or discharging. Consequently, storage technologies can charge and discharge simultaneously, which might result in unrealistic storage operations. To prevent this, we include eq 24 from the work of Elgersma et al.[56] Although this additional constraint

https://doi.org/10.1021/acs.iecr.4c03817
Ind. Eng. Chem. Res. 2025, 64, 4479−4497

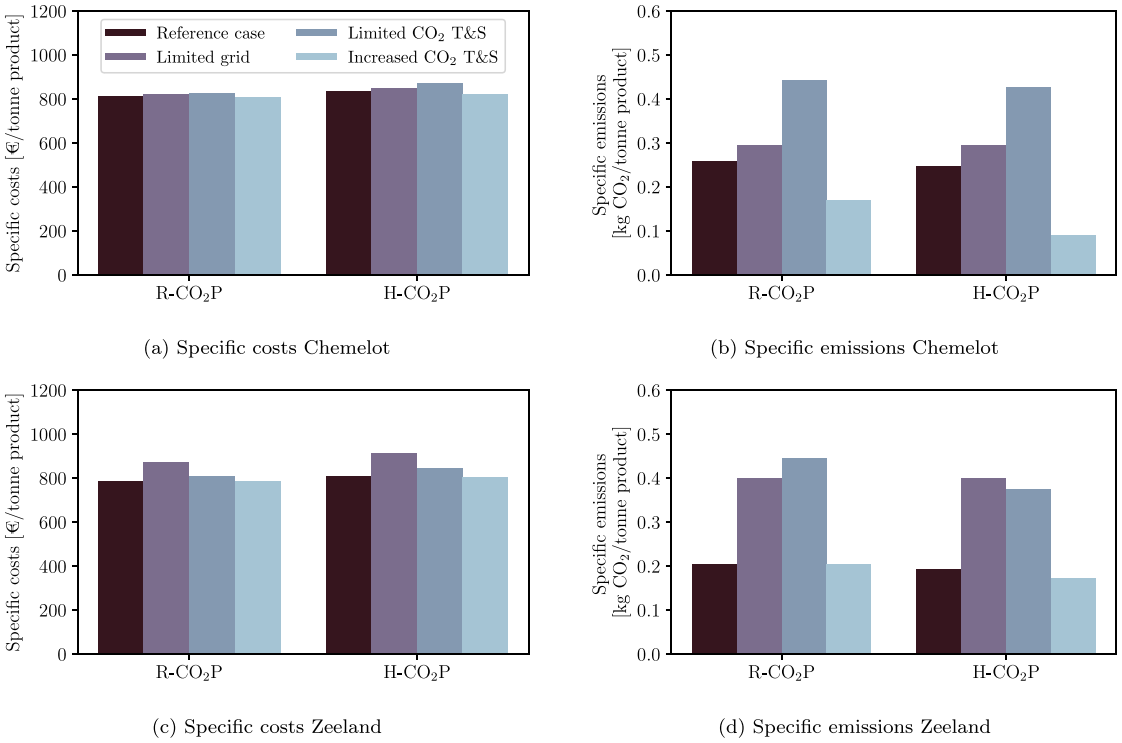

(a) Specific costs Chemelot

(b) Specific emissions Chemelot

(c) Specific costs Zeeland

(d) Specific emissions Zeeland

Figure 6. Specific costs and emissions for the Chemelot and Zeeland clusters under varying grid and CO_2 transport and storage (T&S) capacities. Panels (a) and (b) present the specific costs and emissions for Chemelot, respectively, while panels (c) and (d) show the corresponding values for Zeeland. Results are shown for the reference (R-CO_2P: 150.31 €/t CO_2) and high (H−CO_2P: 250 €/t CO_2) emission price scenarios. The total product quantity includes both the main products (ammonia and ethylene) and all of the byproducts from the naphtha cracker. For reference, current ammonia prices range from 216 to 1049 USD per tonne,[57] while ethylene prices vary between 901 and 1150 USD per tonne.[58]

cannot ensure that $F_{m'',t,h}$ and $P_{m'',t,h}$ are mutually exclusive, the possibility of simultaneous charging and discharging becomes very small.

RESULTS AND DISCUSSION

The optimization framework described above is used to analyze the low-carbon technology deployment, the impact of infrastructure, and the role of flexibility in emissions reduction strategies in the Chemelot and Zeeland clusters. In the following, we present results concerning (i) the optimal cluster design under different CO_2 price scenarios, (ii) the role of access to infrastructures in the transition to low-carbon technologies, (iii) the role of integrating (or not) different processes at the cluster level, and (iv) the role of electrification and technology flexibility for the different processes.

Optimal CO_2 Reduction Strategies. First, we minimized the costs for the Chemelot and Zeeland clusters under two different CO_2 emission price scenarios: a reference price of 150.31 €/t CO_2 and a high price of 250 €/t CO_2. For simplicity, in the following, we refer to these scenarios as R−CO_2P (reference CO_2 price) and H−CO_2P (high CO_2 price), respectively. The minimum-cost optimizations are carried out for Chemelot and Zeeland as independent clusters, i.e., without direct energy and material exchange between the two but considering the optimal integration between the different processes within each respective cluster, e.g., coupling ethylene and ammonia synthesis. Figure 5 presents the optimal system designs and import-export capacities for both clusters under these scenarios. Additional results for the cluster design at different CO_2 prices are presented in Table 6.

We can first identify some general remarks that remain valid independently of location and CO_2 price. It is noteworthy that, in both locations, electric cracking is more favorable than conventional cracking, even with the reference CO_2 emission price. This advantage arises from the inherently lower scope one emissions of electric crackers, particularly when the cracker gas can be used to replace fossil feedstocks in other processes, as seen in this case with syngas reforming and gas-fired boilers. However, it is important to highlight that no emissions reductions would be realized if the cracker gas produced during electric ethylene synthesis were not used to replace other carbon feedstocks within the cluster. The adoption of electric crackers along with the possibility of reuse of cracker gas also affects the choice of hydrogen production process in ammonia production: (electric) syngas reforming is favored over water electrolysis also at higher CO_2 prices due to its ability to utilize the cracker gas as fuel and feedstock. Another common finding for both clusters is that the CO_2 separated from the syngas before NH_3 synthesis is captured and sent to the transport and storage infrastructure. This is not surprising and remains valid as long as (i) the cost of exporting CO_2 is below the CO_2 emission price, and (ii) the CO_2 transport and storage infrastructure is developed as a service to the chemical cluster, i.e. similar to the electric grid.

When comparing the two chemical sites, we can note that the overall cluster capacity and products (NH_3 and C_2H_4) balance are important factors behind the optimal technology selection: provided that Chemelot produces a smaller amount of ammonia compared to ethylene, and given that conventional reforming consumes more cracker gas per tonne of syngas than the eSMR, the optimal combination of syngas production is found by coupling large conventional reformers (~810 MW gas) to small

https://doi.org/10.1021/acs.iecr.4c03817
Ind. Eng. Chem. Res. 2025, 64, 4479−4497

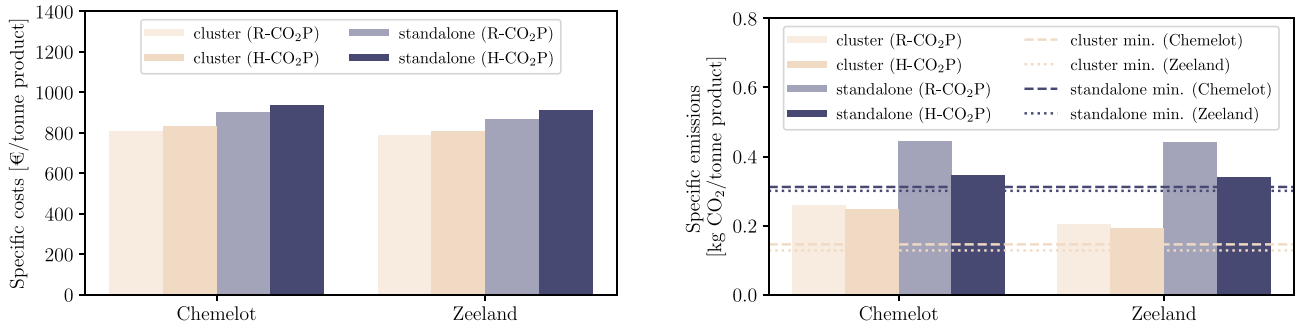

(a) Specific costs (b) Specific emissions

Figure 7. (a) Specific costs and (b) emissions of the Chemelot and Zeeland cluster and standalone cases for the reference (R-CO_2P: 150.31 €/t CO_2) and high (H−CO_2P: 250 €/t CO_2) emission price scenarios. The dashed lines represent the minimum emissions of the systems. Note that the total amount of product includes the main products of the processes (ammonia and ethylene) and all byproducts from the naphtha cracker. Ammonia prices currently range from 216 to 1049 USD per tonne,[57] while ethylene prices vary between 901 and 1150 USD per tonne.[58]

electric ones (~245 MW gas). The remaining cracker gas is used for steam production. On the other hand, in Zeeland, where the ammonia production is larger, syngas reforming is fully electrified. Moreover, the downstream heat consumption is another important driver behind the optimal technology portfolio: in the case of large local heat consumption (i.e., in Zeeland), part of the steam production is electrified as cracking gas can be efficiently reused elsewhere within the cluster battery limits. Finally, as assessed in more detail in the next section, access to CO_2 transport network at the cluster premises plays a key role in the strategies for CO_2 reduction.

The results show that increasing the CO_2 price reduces emissions by 4.5% for Chemelot and 5.5% for Zeeland, with corresponding cost increases of 3.1% and 2.5%, respectively. As for the lower CO_2 price, specific characteristics of the cluster, such as annual production volumes, location, and infrastructure significantly impact the effectiveness of CO_2 reduction strategies: Zeeland achieves greater CO_2 reductions with a smaller cost increase. This is due to its higher CO_2 transport capacity and access to less-expensive and more-abundant green electricity. For both clusters and CO_2 price scenarios, however, the strict capacity limit of the CO_2 transportation pipeline is reached, highlighting once more the importance of connecting the infrastructure for deeper emissions reduction. Further emission reductions are achieved by adopting electric battery systems, which allow better exploiting the variations in the electricity grid and enable electricity storage during low-cost hours (i.e., low CO_2 emissions at moderated electricity price). Due to the tradeoff between savings in operational costs and high investment costs, batteries become competitive only with a high CO_2 emission price. Moreover, due to the increased off-peak hour consumption, the required grid capacity of the cluster can increase significantly, which calls for assessments that go beyond the availability of renewable electricity.

Impact of Critical Infrastructure. The results substantiate the critical role of cluster characteristics in facilitating emission reductions in chemical clusters, particularly concerning the electric grid capacity and CO_2 transport and storage infrastructure. To gain further insight into the significance of this critical infrastructure, three distinct scenarios were evaluated: (1) the anticipated expansion of the electric grid cannot be realized and capacity remains constrained to the current limit (650 MW), (2) the CO_2 transport and storage capacity is unavailable, and (3) the CO_2 transport and storage capacity is increased to 2.5 MT/y for each cluster. Figure 6 shows the resulting specific costs and emissions for these scenarios, and Table S2 in the SI presents the installed capacities.

We find that the specific costs in Chemelot are relatively similar to the reference case, ranging from 1.4% to 4.1% higher in instances of limited grid and CO_2 transport capacity, and up to 1.7% lower in instances of increased CO_2 transport capacity. In contrast, the infrastructure availability in Zeeland has a more pronounced influence on costs: a limited grid capacity leads to a cost increase of 10.8%−13%. This can be attributed to the larger production volume in Zeeland, which requires a significantly larger grid connection for electrification.

In contrast to the limited cost variations, the impact of critical infrastructure on emission reduction potential is significant, particularly regarding CO_2 transport and storage capacity. Without CO_2 sequestration, emissions increase by up to 118% because the CO_2 separated from reformer syngas cannot be stored or further processed. However, increasing transport capacity to 2.5 MT per year reduces emissions by 64% in Chemelot and 10% in Zeeland, compared to the reference case. The results also suggest that the maximum transport capacity of 2.5 MT is not fully utilized, indicating that pipeline capacities of ~2 MT per year for Chemelot and ~2.2 MT per year for Zeeland would be sufficient (under the assumptions made in this study). Limited grid capacity has a smaller yet significant impact on emissions, increasing emissions by 14%−19% in Chemelot and 97%−108% in Zeeland. Moreover, this significantly influences the portfolio of optimal technologies, as for smaller grid connections, eSMR is favored over electric cracking due to its lower electricity consumption. Since eSMR uses less cracker gas than conventional reforming, more cracker gas is exported. Combined with the substitution of electric cracking with conventional cracking, this results in an overall increase in CO_2 production, subsequently raising CO_2 emission costs.

Benefits of Cluster Integration. Next, we assess how process integration within clusters and process interdependencies affect the costs and effectiveness of the overall CO_2 reduction. We compare the optimal cluster results shown above (in the section titled "Optimal CO2 Reduction Strategies") with a scenario in which ammonia and ethylene production are optimized separately, without the possibility of exchanging products or energy. In this standalone scenario, both separate industries have access to half the import and export capacities, and downstream processes are allocated based on the

https://doi.org/10.1021/acs.iecr.4c03817
Ind. Eng. Chem. Res. 2025, 64, 4479−4497

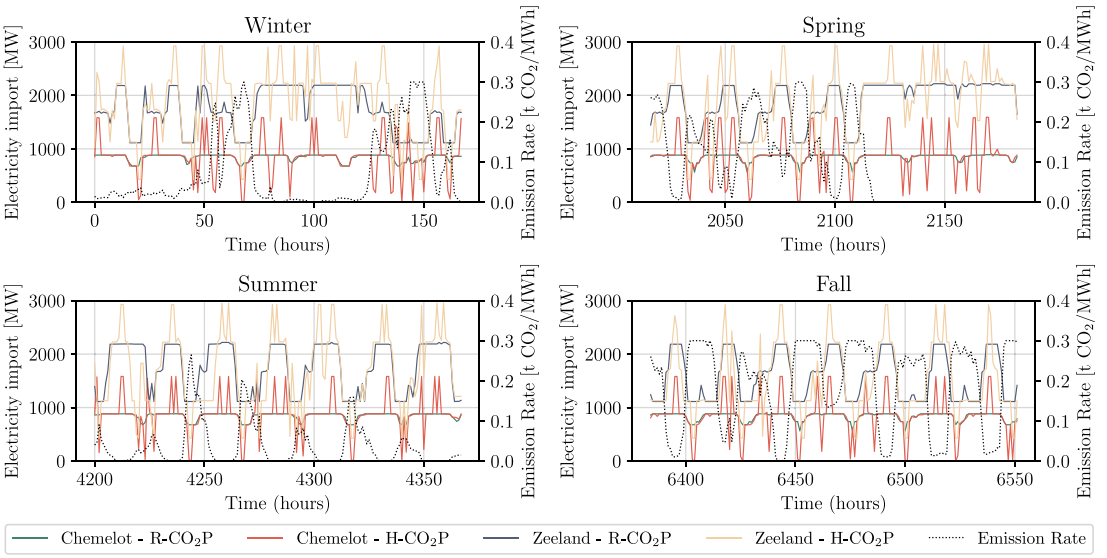

Figure 8. Grid emission rate and the import of electricity in one representative week for each season of the Chemelot and Zeeland cluster for the reference (R-CO_2P: 150.31 €/t CO_2) and high (H−CO_2P: 250 €/t CO_2) emission price scenarios.

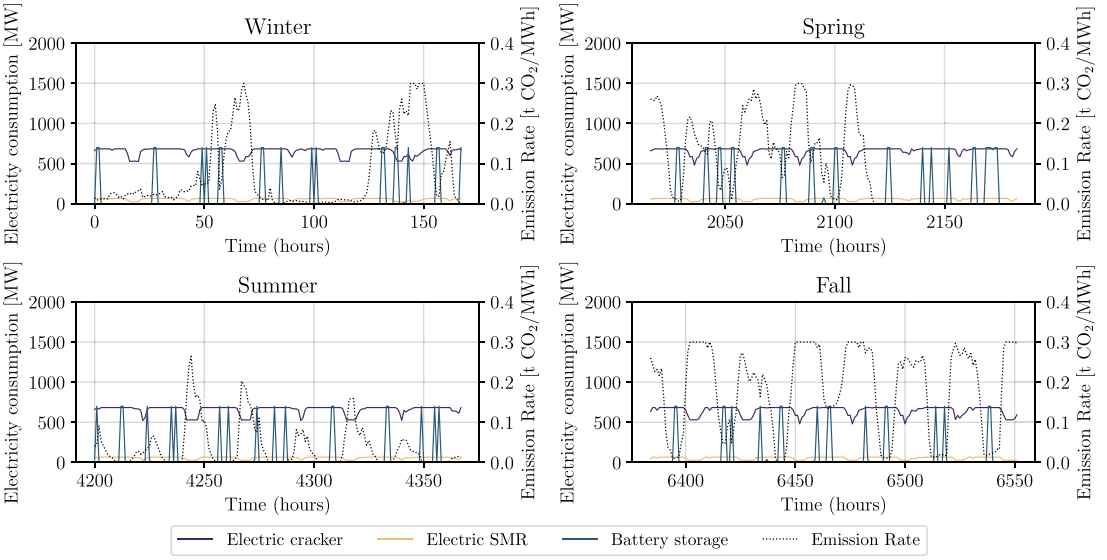

Figure 9. Grid emission rate and electricity consumption profiles of the technologies in one representative week for each season of the Chemelot cluster for the high (H−CO_2P: 250 €/t CO_2) emission price scenario.

industry type. Figure 7 illustrates the specific costs and emissions of the integrated clusters and the standalone scenarios, and Table 6 presents the installed capacities.

Coordinating the transition of all relevant industries at the cluster level benefits both costs and emissions reductions. Notably, cost savings of 9%−11% can be achieved for an integrated cluster compared to the standalone scenario, where the difference results from the CO_2 emission price and cluster location. Emission reductions are even more significant, ranging from 29% to 54%. For our NH_3−C_2H_4 cluster scenario, emissions and cost reduction primarily arise from the possibility of reusing cracker gas available thanks to electrification instead of methane for hydrogen production in the reformer; this lowers the net methane import and, thus, the costs and overall carbon output. Additionally, using cracker gas shifts optimality toward lower CAPEX technologies, e.g., electric reforming instead of electrolysis, while also limiting the overall need for storage.

The results also indicate that the optimal CO_2 reduction strategy for the global cluster is not necessarily optimal for individual industries within the cluster. For instance, while electrification is optimal for ethylene production from a cluster perspective, individual ethylene producers may prefer adopting CC. In the standalone ammonia industry, a combination of eSMR and electrolyzers is adopted to produce hydrogen, while sole reforming is preferred in a cluster to reuse surplus cracker gas. Interestingly, the standalone cost-optimal system design for ammonia leads to lower emissions than those of the ammonia industry in an integrated cluster. This outcome can be attributed to two factors: (1) in the absence of surplus cracker gas, methane must be purchased from the gas grid, making the more feedstock-efficient eSMR and more-flexible electrolyzers preferable, which leads to lower emissions; (2) since exporting cracker gas incurs high emissions (i.e., costs), it is more advantageous to use it within the cluster. As a result, in the Chemelot cluster, the conventional reformer remains the

https://doi.org/10.1021/acs.iecr.4c03817
Ind. Eng. Chem. Res. 2025, 64, 4479−4497

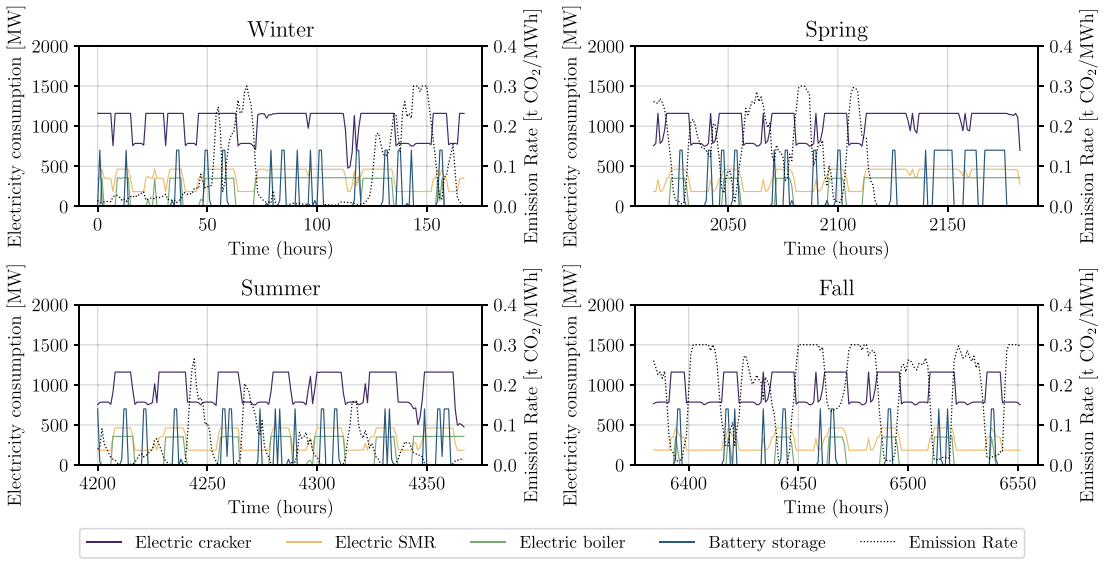

Figure 10. Grid emission rate and electricity consumption profiles of the technologies in one representative week for each season of the Zeeland cluster for the high (H−CO_2P: 250 €/t CO_2) emission price scenario.

optimal and preferred choice over the eSMR due to the smaller scale of ammonia production.

Additionally, we run a minimum emissions optimization (note that all results so far are for minimum costs with two CO_2 price scenarios) for both integrated and standalone clusters (Chemelot and Zeeland). The results show that maximum emission reductions compared to the reference case are 43.4% for Chemelot and 36.8% for Zeeland. Although the reference case already includes some emission reductions compared with the current situation, these findings suggest that achieving a (near) zero-emission chemical cluster is not possible under the assumptions and the technology portfolio considered in this study. Moreover, the absolute minimum emissions of the standalone scenarios are higher than the emissions of the minimum cost results for the clusters. This indicates that the cost-optimal emission reduction potential of an integrated cluster is greater than the maximum emission reduction potential of the two individual industries operating separately.

Electrification and Flexibility. In the absence of a CO_2 transport and storage infrastructure made available at cluster gates, electrification represents the most prominent CO_2 reduction alternative, contingent on the utilization of electricity during periods of low-cost and low carbon intensity. The cumulative distribution of CO_2 intensity, which is shown in Figure 4, indicates that emissions in 2030 are zero for ∼25% of the hours and near zero for 60%−70% of the hours. Consequently, operating electric processes flexibly during these specified hours could potentially achieve a near-zero-emission chemical cluster.

However, Figure 8 shows that in Chemelot, under the reference CO_2 emission price scenario, the timing of electricity imports does not align well with the emission profile and hourly fluctuations in electricity imports are minimal. While a higher CO_2 emission price improves the carbon intensity alignment, Figure 9 illustrates that flexibility is primarily achieved through batteries rather than by adjustment of the operation of primary processes. For example, the electric cracker and reformer are consistently operated near maximum capacity. More specifically, the rationale behind the continuous operation of electric crackers can be attributed to the operational constraints arising from the integration with the conventional SMR, which has little to no flexibility. In contrast, the H−CO_2P scenario in Zeeland exhibits the closest alignment between the timing of the electricity imports and grid emission profiles. As shown in Figure 10, fast power flexibility is provided by batteries and electric boilers, while electrified primary processes, such as the electric cracker, contribute a more gradual power response, typically operating at 30%−50% OE. This implies that, in integrated ethylene−ammonia clusters, flexible electricity consumption can be pursued by adopting more flexible electrified alternatives for both ethylene and ammonia production, though this may require addressing additional investments in storage and potential implications for emissions and resource utilization.

Discussion. Our study indicates that using electrification, carbon capture and storage, and low-carbon hydrogen can cost-effectively reduce emissions under realistic CO_2 emission prices. Notably, we show that what could be regarded as a high CO_2 emission price (250 €/t CO_2) does not necessarily lead to a significant increase in the product-specific cost when multiple complementary technologies for emissions abatement are considered. Importantly, we show that the capability of decreasing CO_2 emissions varies significantly based on the specific characteristics of each chemical cluster: within this context, the availability of critical infrastructure, such as CO_2 transport and storage and electric grid capacity, plays a crucial role. These results suggest that the preferred CO_2 reduction strategy is highly cluster-specific and requires careful analysis and interpretation. Therefore, more detailed optimization models at the cluster level, if required nonlinear and with higher space granularity, can help identify potential scenarios and develop robust CO_2 reduction strategies.

The results indicate that achieving zero scopes one/two emissions in ammonia−ethylene chemical clusters with near-term technologies remains very challenging unless (i) electric input comes with no CO_2 intensity, (ii) no (fossil) carbon-based byproduct is burned, and (iii) access to CO_2 transport and storage is guaranteed for the required maximum nominal capacity. In fact, emissions reduction faces challenges across the full spectrum of scope one, two, and three. The reduction of scope one emission is significantly affected by insufficient access

https://doi.org/10.1021/acs.iecr.4c03817
Ind. Eng. Chem. Res. 2025, 64, 4479−4497

to critical infrastructure (i.e., CO_2 transport) and lack of commercially ready alternatives for deep decarbonization; without CC, emissions can only be partially mitigated in the near-term through the adoption of electric cracking and electrolyzers. On the other hand, eliminating scope two emissions requires the use of electricity exclusively during zero-emission hours, necessitating a substantial grid connection, large electricity storage, and flexible process operation; any of these aspects might be detrimental when missing. Finally, addressing scope three emissions would involve replacing fossil-based feedstocks with biobased or CO_2-neutral alternatives (e.g., direct air capture (DAC)). However, the timely availability of sustainable biomass at scale and of cost-competitive DAC technologies are key limiting factors in the near and midterm future (also note that their analysis was beyond the scope of this study). Additionally, this study focuses exclusively on emissions reduction and does not consider other environmental indicators, such as land or water use, which could be significantly affected by the adoption of some proposed technologies. A comprehensive LCA for the optimal configurations is needed to identify if the proposed solutions are compatible with the different planetary boundaries.

Cluster integration, for instance through the reuse of cracker gas in ammonia production, can enable deeper and more cost-effective emission reductions. However, it limits the potential for flexible operation and, consequently, the ability to better use low-carbon electricity. Although process integration is optimal at the cluster level, system-level benefits may be achieved by pursuing electrification and increasing the level of low-carbon electricity consumption. This also underscores the need to extend the analysis to a broader context, combining national- and cluster-level insights to identify technologies, measures, or electricity prices that encourage flexible operation during low-carbon periods.

As for all models, our framework features several limitations that are worth stressing here. The first limitation of this study is given by model simplifications and by the availability of real-world technology data, especially for complex technologies such as electric crackers and eSMR. For instance, we estimated cost and performance parameters via publicly available data, which are generally less precise than confidential company-specific data, not least due to the unique characteristics of chemical plants. Moreover, in our work, we have neglected the costs associated with the intracluster infrastructure changes, which may add expenses or alter the optimal CO_2 reduction strategy (additional transport costs for cracker gas are expected to be minimal). Similarly, we are considering the reuse of cracker gas to be technically feasible and with no additional costs (although its similarity to CH_4 and syngas reinforces this hypothesis).

Additionally, with this work we are not considering the effect of uncertainties on time- and space-discretized variables that might experience significant changes when varying location and/or year. For example, future feedstock and energy prices are highly uncertain and are prone to fluctuations. This is particularly true for electricity prices, which, in our model, have an hourly resolution rather than an annual average and are influenced by the underlying assumptions of the model used to generate these prices. Although these uncertainties may impact specific aspects and the absolute values of the results, they are not likely to alter the comparative overall conclusions. We provide data and model open access so that the analysis can be easily redone when different values and profiles are available. Furthermore, our analysis neglects the competitive behavior of companies within a cluster, while it assumes full information sharing, which likely overestimates the potential for cluster integration. In reality, much of this information is sensitive and confidential. To enhance modeling outcomes and support decision-making, it is crucial to reduce uncertainties at both the cluster level (e.g., process integration and performance parameters) and the system level (e.g., availability and cost of critical infrastructure). Enhanced information exchange is necessary to identify global optimalities and to ensure the fair distribution of penalties and benefits within the cluster.

CONCLUSIONS AND RECOMMENDATIONS

In this study, we presented an accurate time- and space-discretized MILP formulation to model ammonia-ethylene chemical clusters under varying boundary conditions with hourly resolution over one year. The framework was used to investigate the transition of such clusters toward low CO_2 emissions by using close-to-commercial or commercial technologies, in particular electrified synthesis processes (e.g., electric crackers and SMR), green hydrogen, and carbon capture and storage. In addition to the model framework, which we provide open access, the research makes three key contributions: (1) it identifies optimized near- and midterm CO_2 reduction strategies for chemical clusters, considering multiple industry types and downstream processes, (2) it assesses the role of intracluster process integration and intercluster infrastructure availability, and (3) it evaluates the potential of flexible cluster operation.

Results showed that combining the three different technology pathways allows for a significant decrease in CO_2 emissions. However, access to an increased electricity grid connection and CO_2 transport and storage infrastructure are critical elements of the transition, which may prevent or further improve the reduction potential. Notably, we found that a higher CO_2 emission price can further reduce emissions without affecting the product-specific costs significantly.

Yet, the results also indicate that achieving a zero-emission ammonia−ethylene chemical cluster is not feasible in the near term due to insufficient access to critical infrastructure and to the inherent limit of solutions that do not tackle scope three emissions, i.e., the origin of carbon in the products. Additionally, while process integration can enhance a cluster's overall CO_2 reduction potential, it reduces the potential operational flexibility of electrified processes, thus limiting the capability of exploiting low-carbon electricity. Finally, the findings also reveal that optimal CO_2 reduction strategies are highly cluster-specific and influenced by uncertainties in the cost, performance data, and boundary conditions. This highlights the need for precise yet efficient cluster-level models to identify multiple future scenarios and develop robust CO_2 abatement strategies.

Few additional recommendations can be made. Future research should expand both the spatial and temporal scope while maintaining a detailed analysis at the cluster level. Our findings demonstrate that the surrounding energy system and infrastructure significantly influence a cluster's ability to decarbonize, underscoring the importance of incorporating national system dynamics and decarbonization efforts into cluster-level decision-making. While near-term technologies can reduce emissions cost-effectively, they are insufficient for achieving a zero-emission chemical industry. Consequently, care must be taken to avoid technology lock-in and to find the optimal balance between fast emissions reduction and long-term net-zero achievements. Future research should therefore explore

https://doi.org/10.1021/acs.iecr.4c03817
Ind. Eng. Chem. Res. 2025, 64, 4479−4497

long-term scenarios, considering boundary conditions and advanced technologies necessary for achieving zero-emission chemical clusters, including the mitigation of scope (iii) emissions. The modeling framework presented in this work can potentially integrate detailed cluster-level analysis with national system dynamics while remaining computationally efficient enough to assess long-term deep decarbonization strategies for chemical clusters.

■ ASSOCIATED CONTENT

Supporting Information

The Supporting Information is available free of charge at https://pubs.acs.org/doi/10.1021/acs.iecr.4c03817.

Additional information regarding the downstream processes, the collection of cost and performance data, and the justification for using 20 design days (PDF)
(ZIP)

■ AUTHOR INFORMATION

Corresponding Author

Matteo Gazzani − *Copernicus Institute of Sustainable Development, Utrecht University, Utrecht 3584 CB, The Netherlands; Sustainable Process Engineering Chemical Engineering and Chemistry, Eindhoven University of Technology, Eindhoven 5612 AP, The Netherlands;* orcid.org/0000-0002-1352-4562; Email: m.gazzani@uu.nl

Authors

Julia L. Tiggeloven − *Copernicus Institute of Sustainable Development, Utrecht University, Utrecht 3584 CB, The Netherlands; TNO, Energy Transition Studies, Amsterdam 1030 CE, The Netherlands*

André P. C. Faaij − *Copernicus Institute of Sustainable Development, Utrecht University, Utrecht 3584 CB, The Netherlands; TNO, Energy Transition Studies, Amsterdam 1030 CE, The Netherlands*

Gert Jan Kramer − *Copernicus Institute of Sustainable Development, Utrecht University, Utrecht 3584 CB, The Netherlands*

Complete contact information is available at: https://pubs.acs.org/10.1021/acs.iecr.4c03817

Notes

The authors declare no competing financial interest.

■ ACKNOWLEDGMENTS

We thank Charidimos Makrakis (former Energy Science student of Utrecht University) for his contribution to the initial data collection on the ammonia industry, and Sander Blom (TNO) for providing the electricity prices and carbon intensity data.

■ LIST OF ABBREVIATIONS

AEC = alkaline electrolysis cell
ASU = air separation unit
ATR = autothermal reforming
CAPEX = capital expenditures
CEPCI = Chemical Engineering Plant Cost Index
CC = carbon capture
DAC = direct air capture
DD = design day
eSMR = electric steam methane reforming
HB = Haber Bosch
MDEA = methyldiethanolamine
MEA = monoethanolamine
MILP = mixed-integer linear programming
OE = operation envelope
RT = ramping time
SI = Supporting Information
SMR = steam methane reforming
TSAM = time series aggregation module
T&S = transport and storage
WGS = water gas shift
WSP = warm standby power

■ LIST OF MATHEMATICAL SYMBOLS

Indices

$d \in \mathcal{D}$ = set of design days
$h \in \mathcal{H}$ = set of clusters
$k \in \mathcal{K}$ = set of timesteps per day
$m \in \mathcal{M}$ = set of technologies
$m' \in \mathcal{M}'$ = subset of medium-dynamic technologies
$m'' \in \mathcal{M}''$ = subset of storage technologies
$n \in \mathcal{N}$ = set of carriers
$n' \in \mathcal{N}'$ = subset of plant output carriers
$n'' \in \mathcal{N}''$ = subset of plant input carriers
$t \in T$ = set of timesteps

Variables

C = total annual system costs
D = carrier demand
E = total system emissions
F = consumption of technology
g = binary charging storage technology
I = carrier import
J = carrier export
L = storage level
P = production of technology
S = technology size
x = binary on/off status plant

Parameters

α = conversion efficiency plant
β = input ratio plant
c^{pipeline} = cost of kilometer pipeline
c^{storage} = cost of a tonne offshore CO_2 storage
d = distance to Rotterdam
γ = minimum feasible operating point
ε = emission factor electricity grid
ζ = size-independent cost parameter
η^{C}, η^{D} = charging and discharging efficiencies
θ = CO_2 tax
ι = import price
κ = emission factor technology
λ = size-dependent cost parameter
ν = CO_2 transport and storage cost
σ = sequence of design days
ϕ = warm standby power fraction
ψ = maintenance cost fraction
ω = annuity factor

Other

A = constraint matrix continuous variables
B = constraint matrix binary variables
f = objective function
N = dimensionality of variables

https://doi.org/10.1021/acs.iecr.4c03817
Ind. Eng. Chem. Res. 2025, 64, 4479−4497

b = constraint known term

REFERENCES

(1) Gabrielli, P.; Rosa, L.; Gazzani, M.; Meys, R.; Bardow, A.; Mazzotti, M.; Sansavini, G. Net-zero emissions chemical industry in a world of limited resources. *One Earth* **2023**, *6*, 682−704.

(2) Bauer, F.; Tilsted, J. P.; Pfister, S.; Oberschelp, C.; Kulionis, V. Mapping GHG emissions and prospects for renewable energy in the chemical industry. *Curr. Opin. Chem. Eng.* **2023**, *39*, 100881.

(3) IEA Tracking Clean Energy Progress 2023. 2023; License: CC BY 4.0.

(4) Woodall, C. M.; Fan, Z.; Lou, Y.; Bhardwaj, A.; Khatri, A.; Agrawal, M.; Mccormick, C. F.; Friedmann, S. J. Technology options and policy design to facilitate decarbonization of chemical manufacturing. *Joule* **2022**, *6*, 2474−2499.

(5) Hackl, R.; Harvey, S. Framework methodology for increased energy efficiency and renewable feedstock integration in industrial clusters. *Appl. Energy* **2013**, *112*, 1500−1509.

(6) Theo, W. L.; Lim, J. S.; Wan Alwi, S. R.; Mohammad Rozali, N. E.; Ho, W. S.; Abdul-Manan, Z. An MILP model for cost-optimal planning of an on-grid hybrid power system for an eco-industrial park. *Energy* **2016**, *116*, 1423−1441.

(7) Janipour, Z.; de Nooij, R.; Scholten, P.; Huijbregts, M. A.; de Coninck, H. What are sources of carbon lock-in in energy-intensive industry? A case study into Dutch chemicals production. *Energy Res. Soc. Sci.* **2020**, *60*, 101320.

(8) Janipour, Z.; de Gooyert, V.; Huijbregts, M.; de Coninck, H. Industrial clustering as a barrier and an enabler for deep emission reduction: a case study of a Dutch chemical cluster. *Clim. Policy* **2022**, *22*, 320−338.

(9) Schneider, C.; Lechtenböhmer, S.; Samadi, S. Risks and opportunities associated with decarbonising Rotterdams industrial cluster. *Environ. Innovation Soc. Trans.* **2020**, *35*, 414−428.

(10) Sovacool, B. K.; Geels, F. W.; Iskandarova, M. Industrial clusters for deep decarbonization. *Science* **2022**, *378*, 601−604.

(11) Gunawan, T. A.; Luo, H.; Greig, C.; Larson, E. Shared CO_2 capture, transport, and storage for decarbonizing industrial clusters. *Appl. Energy* **2024**, *359*, 122775.

(12) Küng, L.; Strunge, T.; Sunny, N.; Nie, Z.; Tariq, N.; Korre, A.; Shah, N.; Van der Spek, M. An open-source toolkit to design and evaluate net-zero pathways for industrial clusters. In *Proceedings of the 16th Greenhouse Gas Control Technologies Conference (GHGT-16)*, Oct. 23−24, 2022, .

(13) Namazifard, N.; Vingerhoets, P.; Delarue, E. Long-term cost optimization of a national low-carbon hydrogen infrastructure for industrial decarbonization. *Int. J. Hydrogen Energy* **2024**, *64*, 583−598.

(14) Ibrahim, Y.; Al-Mohannadi, D. M. Optimization of low-carbon hydrogen supply chain networks in industrial clusters. *Int. J. Hydrogen Energy* **2023**, *48*, 13325−13342.

(15) Giannikopoulos, I.; Skouteris, A.; Allen, D. T.; Baldea, M.; Stadtherr, M. A. Thermal Electrification of Chemical Processes Using Renewable Energy: Economic and Decarbonization Impacts. *Ind. Eng. Chem. Res.* **2024**, *63*, 12064−12082.

(16) El Wajeh, M.; Mhamdi, A.; Mitsos, A. Optimal Design and Flexible Operation of a Fully Electrified Biodiesel Production Process. *Ind. Eng. Chem. Res.* **2024**, *63*, 1487−1500.

(17) Samadi, S.; Schneider, C.; Lechtenböhmer, S. Deep decarbonisation pathways for the industrial cluster of the Port of Rotterdam. *ECEEE Ind. Summer Study* **2018**, 399−409.

(18) Fleiter, T.; Rehfeldt, M.; Herbst, A.; Elsland, R.; Klingler, A. L.; Manz, P.; Eidelloth, S. A methodology for bottom-up modelling of energy transitions in the industry sector: The FORECAST model. *Energy Strategy Rev.* **2018**, *22*, 237−254.

(19) Berghout, N.; Meerman, H.; van den Broek, M.; Faaij, A. Assessing deployment pathways for greenhouse gas emissions reductions in an industrial plant − A case study for a complex oil refinery. *Appl. Energy* **2019**, *236*, 354−378.

(20) Yáñez, E.; Meerman, H.; Ramírez, A.; Castillo, E.; Faaij, A. Fully integrated CO_2 mitigation strategy for an existing refinery: A case study in Colombia. *Appl. Energy* **2022**, *313*, 118771.

(21) Eerens, H.; Dam, D. V. *Decarbonisation options for Large Volume Organic Chemicals production*; DOW: Terneuzen, 2022. Available via the Internet at: www.pbl.nl/en, accessed March 19, 2024.

(22) Batool, M.; Wetzels, W. *Decarbonization options for the Dutch fertilizer industry*. 2019. Available via the Internet at: https://www.pbl.nl/en, accessed March 19, 2024.

(23) Oliveira, C.; Dril, A. W. N. *Decarbonisation options for Large Volume Organic Chemicals production*; SABIC Geleen2021. Available via the Internet at: www.pbl.nl/en., accessed March 19, 2024.

(24) Dutch Emissions Authority Tarieven CO_2-heffing. Available via the Internet at: https://www.emissieautoriteit.nl/onderwerpen/tarieven-co2-heffing, accessed June 21, 2024.

(25) Ren, T.; Patel, M.; Blok, K. Olefins from conventional and heavy feedstocks: Energy use in steam cracking and alternative processes. *Energy* **2006**, *31*, 425−451.

(26) Weimann, L.; Dubbink, G.; van der Ham, L.; Gazzani, M. A thermodynamic-based mixed-integer linear model of post-combustion carbon capture for reliable use in energy system optimization. *Appl. Energy* **2023**, *336*, 120738.

(27) Tiggeloven, J. L.; Faaij, A. P.; Kramer, G. J.; Gazzani, M. Optimization of Electric Ethylene Production: Exploring the Role of Cracker Flexibility, Batteries, and Renewable Energy Integration. *Ind. Eng. Chem. Res.* **2023**, *62*, 16360−16382.

(28) From, T. N.; Partoon, B.; Rautenbach, M.; Østberg, M.; Bentien, A.; Aasberg-Petersen, K.; Mortensen, P. M. Electrified steam methane reforming of biogas for sustainable syngas manufacturing and next-generation of plant design: A pilot plant study. *Chem. Eng. J.* **2024**, *479*, 147205.

(29) Balakotaiah, V.; Ratnakar, R. R. Modular reactors with electrical resistance heating for hydrocarbon cracking and other endothermic reactions. *AlChE J.* **2022**, *68*, e17542.

(30) Wismann, S. T.; Engbæk, J. S.; Vendelbo, S. B.; Bendixen, F. B.; Eriksen, W. L.; Aasberg-Petersen, K.; Frandsen, C.; Chorkendorff, I.; Mortensen, P. M. Electrified methane reforming: A compact approach to greener industrial hydrogen production. *Science* **2019**, *364*, 756−759.

(31) Armijo, J.; Philibert, C. E. Flexible production of green hydrogen and ammonia from variable solar and wind energy: Case study of Chile and Argentina. *Int. J. Hydrogen Energy* **2020**, *45*, 1541−1558.

(32) Alvarez, S. *Teslás giant Moss Landing Megapack battery storage project: How is it doing now?*, 2022. Available via the Internet at: https://www.teslarati.com/tesla-moss-landing-megapack-battery-latest-updates-incidents/, accessed March 19, 2024.

(33) Rijksoverheid Windenergiegebied Hollandse Kust (west) - Wind op zee, 2022. Available via the Internet at: https://windopzee.nl/imagemaps/kaart-waar-wanneer/hollandse-kust-west/, accessed March 9, 2024.

(34) Koirala, B.; Hers, S.; Morales-España, G.; Özdemir, O.; Sijm, J.; Weeda, M. Integrated electricity, hydrogen and methane system modelling framework: Application to the Dutch Infrastructure Outlook 2050. *Appl. Energy* **2021**, *289*, 116713.

(35) Tennet/Gasunie. Scenario's investeringsplannen 2024, 2023. Available via the Internet at: https://www.tennet.eu/nl/over-tennet/publicaties/investeringsplannen, accessed June 20, 2024.

(36) ENTSO-E Ten-Year Network Development Plan (TYNDP) Scenarios Report, 2020. Available via the Internet at: https://2020.entsos-tyndp-scenarios.eu/download-data/, accessed March 19, 2024.

(37) Cluster Energie Strategie 2022 Chemelot 2030−2050, 2022. Available via the Internet at: https://www.chemelot.nl/duurzaamheid/cluster-energie-strategie-chemelot-2030-2050, accessed March 19, 2024.

(38) Smart Delta Resources and Witteveen+Bos Cluster Energie Strategie (CES) Schelde-Deltaregio.2022. Available via the Internet at: https://www.smartdeltaresources.com/sites/default/files/inline-files/SDR-CES%201.0.pdf, accessed March 19, 2024.

(39) INSEE International prices of imported raw materials - Naphtha (European Northwest) - Spot price in US dollars per tonne, 2022.

https://doi.org/10.1021/acs.iecr.4c03817
Ind. Eng. Chem. Res. 2025, 64, 4479−4497

Available via the Internet at: https://www.insee.fr/en/statistiques/serie/010002081#Tableau, Accessed July 17, 2024.
(40) Wetzels, W.; Luteijn, G. *Scenario's voor aardgas- en elektriciteitsprijzen voor kleinverbruikers in de periode 2025−2040*, 2023. Available via the Internet at: https://www.pbl.nl/kev/publicaties, accessed March 19, 2024.
(41) Fuller, J.; Spence, E. *Porthos CCS − Transport and Storage (T&S) Tariff Review*, 2020. Available via the Internet at: https://zoek.officielebekendmakingen.nl/blg-947442.pdf, accessed March 19, 2024.
(42) Wiegner, J. F.; Tiggeloven, J. L.; Bertoni, L.; Ossentjuk, I. *UU-ER/AdOpT-NET0: v0.1.3*. 2024; DOI: 10.5281/zenodo.13384688.
(43) Geidl, M.; Koeppel, G.; Favre-Perrod, P.; Klöckl, B.; Andersson, G.; Fröhlich, K. Energy hubs for the future. *IEEE Power Energy Mag.* **2007**, *5*, 24.
(44) Gurobi Gurobi Optimization LLC, Gurobi, version 11. Available via the Internet at: http://www.gurobi.com,2000; accessed June 20, 2024.
(45) *IEAGHG Techno-Economic Evaluation of HYCO Plant integrated to Ammonia/Urea or Methanol Production with CCS*; Report, 2017.
(46) *IEAGHG Low-Carbon Hydrogen from Natural Gas: Global Roadmap*; Report, 2022
(47) DEA Technology Data for Renewable Fuels, 2017. Available via the Internet at: http://www.ens.dk/teknologikatalog, accessed March 19, 2024.
(48) Arnaiz del Pozo, C.; Cloete, S. Techno-economic assessment of blue and green ammonia as energy carriers in a low-carbon future. *Energy Convers. Manage.* **2022**, *255*, 115312.
(49) Papadias, D. D.; Peng, J.-K.; Ahluwalia, R. K. *H2@Scale: Outlook of Hydrogen Carriers at Different Scales*. Presented at the Department of Energy Hydrogen Carriers Workshop: Novel Pathways for Optimized Hydrogen Transport Stationary Storage, Denver, CO, November 13−14, **2019**.
(50) Roussanaly, S.; Deng, H.; Skaugen, G.; Gundersen, T. At what pressure shall CO_2 be transported by ship? An indepth cost comparison of 7 and 15 barg shipping. *Energies* **2021**, *14*.5635
(51) Gardarsdottir, S. O.; De Lena, E.; Romano, M.; Roussanaly, S.; Voldsund, M.; Pérez-Calvo, J.-F.; Berstad, D.; Fu, C.; Anantharaman, R.; Sutter, D.; et al. Comparison of technologies for CO2 capture from cement production—Part 2: Cost analysis. *Energies* **2019**, *12*, 542.
(52) DEA Technology Data-Energy storage, 2022. Available via the Internet at: http://www.ens.dk/teknologikatalog, accessed March 14, 2024.
(53) IRENA Electricity storage and renewables: costs and markets to 2030, 2017. Available via the Internet at: https://www.irena.org/publications/2017/Oct/Electricity-storage-and-renewables-costs-and-markets.
(54) Kotzur, L.; Hoffmann, M. *TSA: Time Series Aggregation Module*. https://tsam.readthedocs.io/en/latest/, 2023; accessed June 14, 2024.
(55) Gabrielli, P.; Gazzani, M.; Martelli, E.; Mazzotti, M. Optimal design of multi-energy systems with seasonal storage. *Appl. Energy* **2018**, *219*, 408−424.
(56) Elgersma, M. B.; Morales-España, G.; Aardal, K. I.; Helistö, N.; Kiviluoma, J.; de Weerdt, M. M. *Tight MIP Formulations for Optimal Operation and Investment of Storage Including Reserves*, 2024. Available via the Internet at: https://arxiv.org/html/2411.17484, accessed November 28, 2024.
(57) IEA Indicative production costs for ammonia via electrolysis in selected regions compared to current references, 2023. Available via the Internet at: https://www.iea.org/data-and-statistics/charts/indicative-production-costs-for-ammonia-via-electrolysis-in-selectedregions-compared-to-current-references, accessed September 3, 2023.
(58) IEA Annual ethylene capacity/demand growth and regional price developments, 2015−2020,2019. Available via the Internet at: https://www.iea.org/data-and-statistics/charts/annual-ethylene-capacity-demand-growth-and-regional-price-developments-2015-2020; Accessed on 2024−09−03.

https://doi.org/10.1021/acs.iecr.4c03817
Ind. Eng. Chem. Res. 2025, 64, 4479−4497